report of the Clinical Advisory Committee meeting-Airlie House, Virginia, November 1997. *J Clin Oncol* 1999; **17**: 3835–3849.
11 Malcovati L, Germing U, Kuendgen A, Porta D, Pascutto C, Inverinizzi R *et al.* Time-dependent prognostic scoring system for predicting survival and leukemic evolution in myelodysplastic syndromes. *J Clin Oncol* 2007; **25**: 3503–3510.
12 Bennett JM, Catovsky D, Daniel MT, Flandrin G, Galton DA, Gralnick HR *et al.* Proposals for the classification of the myelodysplastic syndromes. *Br J Haematol* 1982; **51**: 189–199.
13 Dastugue N, Payen C, Lafage-Pochitaloff M, Bernard P, Leroux D, Huguet-Rigal F *et al.* Prognostic significance of karyotype in *de novo* adult acute myeloid leukemia. The BGMT group. *Leukemia* 1995; **9**: 1491–1498.
14 Mauritzson N, Johansson B, Albin M, Rylander L, Billstrom R, Ahlgren T *et al.* Survival time in a population-based consecutive series of adult acute myeloid leukemia the prognostic impact of karyotype during the time period 1976–1993. *Leukemia* 2000; **14**: 1039–1043.
15 Grimwade D, Walker H, Oliver F, Wheatley K, Harrison C, Harrison G *et al.* The importance of diagnostic cytogenetics on outcome in AML: analysis of 1612 patients entered into the MRC AML 10 trial. The Medical Research Council Adult and Children's Leukaemia Working Parties. *Blood* 1998; **92**: 2322–2333.
16 Hasle H, Alonzo TA, Auvrignon A, Behar C, Chang M, Creutzig U *et al.* Monosomy 7 and deletion 7q in children and adolescents with acute myeloid leukemia: an international retrospective study. *Blood* 2007; **109**: 4641–4647.
17 Morel P, Hebbar M, Lai JL, Duhamel A, Preudhomme C, Wattel E *et al.* Cytogenetic analysis has strong independent prognostic value in *de novo* myelodysplastic syndromes and can be incorporated in a new scoring system: a report on 408 cases. *Leukemia* 1993; **7**: 1315–1323.
18 Toyama K, Ohyashiki K, Yoshida Y, Abe T, Asano S, Hirai H *et al.* Clinical implications of chromosomal abnormalities in 401 patients with myelodysplastic syndromes: a multicentric study in Japan. *Leukemia* 1993; **7**: 499–508.
19 Jacobs RA, Cornbleet M, Vardiman J, Larson R, LeBeau MM, Rowley JD. Prognostic implications of morphology and karyotype in primary myelodysplastic syndromes. *Blood* 1986; **67**: 1765–1772.
20 Yunis JJ, Lobell M, Arnesen MA, Oken MM, Mayer MG, Rydell RE *et al.* Refined chromosome study helps define prognostic subgroups in most patients with primary myelodysplastic syndrome and acute myelogenous leukaemia. *Br J Haematol* 1988; **68**: 189–194.
21 Pierre R, Catovsky D, Mufti G, Swansbury G, Mecucci C, Dewald GW *et al.* Clinical cytogenetic correlations in myelodysplasia (preleukemia). *Cancer Genet Cytogenet* 1989; **40**: 149–161.
22 Samuels BL, Larson RL, LeBeau MM, Daly KM, Bitter MA, Vardiman JW *et al.* Specific chromosomal abnormalities in acute nonlymphocytic leukemia correlate with drug susceptibility *in vivo*. *Leukemia* 1988; **2**: 79–83.
23 Kardos G, Baumann I, Passmore SJ, Locatelli F, Hasle H, Schultz KR *et al.* Refractory anemia in childhood: a retrospective analysis of 67 patients with particular reference to monosomy 7. *Blood* 2003; **102**: 1997–2003.
24 Lee JH, Lee JH, Shin YR, Lee JS, Kim WK, Chi HS *et al.* Application of different prognostic scoring systems and comparison of the FAB and WHO classifications in Korean patients with myelodysplastic syndrome. *Leukemia* 2003; **17**: 305–313.
25 Chen B, Zhao WL, Jin J, Xue YQ, Cheng X, Chen XT *et al.* Clinical and cytogenetic features of 508 Chinese patients with myelodysplastic syndrome and comparison with those in Western countries. *Leukemia* 2005; **19**: 767–775.
26 Sokal G, Michaux JL, van den Berghe H, Cordier A, Rodhain J, Ferrantr A *et al.* A new hematologic syndrome with a distinct karyotype: the 5q- chromosome. *Blood* 1975; **46**: 519–533.
27 Dewald GW, Davis MP, Pierre RV, O'Fallon JR, Hoagland HC. Clinical characteristics and prognosis of 50 patients with a myeloproliferative syndrome and deletion of part of the long arm of chromosome 5. *Blood* 1985; **66**: 189–197.
28 Haase D, Germing U, Schanz J, Pfeilstöcker M, Nösslinger T, Hildebrandt B *et al.* New insights into the prognostic impact of the karyotype in MDS and correlation with subtypes: evidence from a core dataset of 2124 patients. *Blood* 2007; **110**: 4385–4395.
29 Malcovati L, Porta MG, Pascutto C, Invernizzi R, Boni M, Travaglino E *et al.* Prognostic factors and life expectancy in myelodysplastic syndromes classified according to WHO criteria: a basis for clinical decision making. *J Clin Oncol* 2005; **23**: 7594–7603.
30 List AF, Baker AF, Green S, Bellamy W. Lenalidomide: targeted anemia therapy for myelodysplastic syndromes. *Cancer Control* 2006; **13**: 4–11.

Supplementary Information accompanies the paper on the Leukemia website (http://www.nature.com/leu)

Biology of Blood and Marrow Transplantation 14:268-281 (2008)
© 2008 American Society for Blood and Marrow Transplantation
1083-8791/08/1403-0001$32.00/0
doi:10.1016/j.bbmt.2007.12.004

ASBMT
American Society for Blood and Marrow Transplantation

Growth and Differentiation Advantages of CD4$^+$OX40$^+$ T Cells from Allogeneic Hematopoietic Stem Cell Transplantation Recipients

Takero Shindo, Takayuki Ishikawa, Akiko Fukunaga, Toshiyuki Hori, Takashi Uchiyama

Department of Hematology and Oncology, Graduate School of Medicine, Kyoto University, Kyoto, Japan

Correspondence and reprint requests: Takayuki Ishikawa, MD, Department of Hematology and Oncology, Graduate School of Medicine, Kyoto University, 54 Shogoin-Kawaracho, Sakyo-ku, Kyoto 606-8507, Japan (e-mail: tishi@kuhp.kyoto-u.ac.jp).

Received June 28, 2007; accepted December 5, 2007

ABSTRACT

OX40 (CD134), an activation-induced costimulatory molecule, is mainly expressed on CD4$^+$ T cells. Several reports, including previous reports from our laboratory, suggest that OX40-mediated signaling plays an important role in the development of graft-versus-host disease (GVHD) after allogeneic hematopoietic stem cell transplantation (Allo HSCT). Here, we show that peripheral blood CD4$^+$OX40$^+$ T cells are a unique cell subset as they possess the homing receptors of lymph nodes, and some of them have an exceptional capacity to produce high levels of interleukin-2 (IL-2) upon the stimulation through T cell receptors. Stimulation with IL-7 acts selectively on CD4$^+$OX40$^+$ T cells not only to induce antigen-independent growth but also to increase the frequency of cells with IL-2-producing potential. Simultaneous, but not sequential, ligation of the T cell receptor and OX40 induces CD4$^+$OX40$^+$ T cells to produce far more IL-2, which causes them to proliferate abundantly and differentiate readily into Th1- or Th2-biased effector memory T cells, especially in Allo HSCT recipients. Although not all the CD4$^+$OX40$^+$ T cells had IL-2-producing capacity, Allo HSCT recipients with chronic GVHD (cGVHD) had a significantly higher frequency of IL-2-producing OX40$^+$ cells in their peripheral blood CD4$^+$ T cell subset than Allo HSCT recipients without cGVHD. Collectively, CD4$^+$OX40$^+$ T cells with IL-2-producing potential are expected to be privileged for growth and differentiation in lymph nodes upon antigen presentation, suggesting that they might be involved in the process of inducing or maintaining cGVHD.
© 2008 American Society for Blood and Marrow Transplantation

KEY WORDS

OX40 • CD4 T cell • Allogeneic hematopoietic stem cell transplantation • Chronic graft-versus-host disease (GVHD)

INTRODUCTION

Chronic graft-versus-host disease (cGVHD) remains a serious complication that affects long-term survivors of allogeneic hematopoietic stem cell transplantation (Allo HSCT). It is not only the leading cause of nonrelapse mortality (NRM), it is also associated with decreased quality of life [1]. To prevent and treat GVHD, immunosuppressive agents such as calcineurin inhibitors are generally used, which increases the risk of developing opportunistic infections. It has been shown that GVHD is initiated by donor-derived CD4$^+$ and CD8$^+$ T cells that recognize a subset of host antigens [2,3]. Indeed, it has been shown that ex vivo depletion of the T cells in the graft effectively reduces the incidence and severity of acute GVHD (aGVHD) [4,5]. Unfortunately, this technique is also associated with increased incidences of graft rejection, relapses, and infectious complications, which prevents it from being widely used. Another technique to specifically deplete donor-derived alloreactive T cells that is currently being developed involves stimulating the graft with recipient cells in vitro and then depleting the activated T cells with monoclonal antibodies (mAb) [6-8]. However, such depletion-based techniques would probably fail to prevent cGVHD because the alloreactive T cells that cause cGVHD are believed to be derived from hematopoietic stem cells (HSC) in the graft rather than already being mature T cells [9-12]. A better way to prevent and treat

cGVHD would be to first identify which alloreactive cells are directly responsible for this disease; these cells could then be readily detected in the blood and specifically depleted within the host.

OX40 (CD134) is a member of the tumor necrosis factor (TNF) receptor superfamily [13], and is an activation-induced antigen that is predominantly expressed on CD4$^+$ T cells [14]. The ligand for OX40 (OX40L) is mainly expressed on activated antigen-presenting cells (APCs) such as dendritic cells and B cells [15-17]. OX40 signaling acts as an important costimulatory signal, as it augments interleukin 2 (IL-2) production [18,19], prolongs cell survival by upregulating Bcl-2 and Bcl-x_L expression [20], induces the clonal expansion of naïve CD4$^+$ T cells [19,21], and generates memory T cells by promoting the survival of effector T cells [19,22,23]. OX40-mediated signaling is also indispensable for expanding memory T cells in secondary immune responses and prolonging their survival [24]. A large body of evidence suggests that OX40-mediated signaling plays a pivotal role in the development of several immune-mediated conditions such as experimental autoimmune encephalomyelitis [16,25], collagen-induced arthritis [26], allergic lung inflammation [24,27], inflammatory bowel disease [28], and GVHD [29,30]. Because the in vivo blockade of OX40-mediated signals ameliorates these diseases in murine models, it is possible that targeting OX40 may also be useful for treating human diseases [14].

Buenafe et al [31] reported that the antigen-specific T cells in the spinal cord of Lewis rats displaying experimental autoimmune encephalomyelitis are frequently CD4$^+$OX40$^+$ T cells. Tittle et al [32] showed that CD4$^+$OX40$^+$ T cells are the alloreactive T cells in a murine GVHD model. In addition, we previously showed that the occurrence of cGVHD correlates positively with the frequency of peripheral blood CD4$^+$OX40$^+$ T cells [33]. Consequently, we speculated that the circulating CD4$^+$OX40$^+$ T cell subset of Allo HSCT recipients contains alloreactive T cells that are involved in the process of inducing and maintaining cGVHD. To further understand the role CD4$^+$OX40$^+$ T cells play in the development of cGVHD, we here isolated the CD4$^+$OX40$^+$ T cells from Allo HSCT recipients and healthy volunteers (HVs) and assessed their characteristics.

SUBJECTS, MATERIALS, AND METHODS

Subjects

Peripheral blood samples were obtained from 13 HVs and 43 Allo HSCT recipients who had undergone transplantation at least 100 days previously. Each subject gave written informed consent. Allo HSCT recipients were required to be in complete donor chimerism as well as in complete remission at the time of sampling. The clinical characteristics of the Allo HSCT recipients are summarized in Table 1. Standard conditioning for patients with hematologic malignancies consisted of 12 Gy total-body irradiation (TBI) and cyclophosphamide (Cy; 120 mg/kg), 12 Gy TBI and melphalan (Mel; 140 mg/m^2), or busulfan (Bu/Cy; 16 mg/kg) and Cy (120 mg/kg). Patients with aplastic anemia (AA) received 200 mg/kg Cy and antithymocyte-globulin (ATG), and a patient with adrenoleukodystrophy was treated with Bu (8 mg/kg), Cy (120 mg/kg), and 7.5Gy total lymphoid irradiation [34]. Reduced-intensity conditioning (RIC) was performed using 2-4 Gy TBI, fludarabine (Flu; 125 mg/m^2), and either Bu (8 mg/kg) or Mel (80-140 mg/m^2). The presence of cGVHD in Allo HSCT recipients was defined as the presence of active symptoms, for which immunosuppressive therapy was required [1,35]. In other words, patients defined as positive for cGVHD included patients with extensive cGVHD and patients with limited cGVHD, which manifests itself as significant hepatic dysfunction (value of Alkaline Phosphatase greater than twice the normal upper limit). All studies involving these blood samples were approved by the institutional review board of Kyoto University.

Table 1. *Patient Characteristics*

Characteristics	Data
No. male/no. female	20/23
Median age, years (range)	52 (25-74)
Diagnosis, no. (%)	
Acute lymphoblastic leukemia	2 (5)
Acute myelogenous leukemia	12 (28)
Myelodysplastic syndrome	7 (16)
CML/MPD	7 (16)
Adult T cell Leukemia	1 (2)
Lymphoma	8 (19)
Myeloma	3 (7)
Aplastic anemia	2 (5)
Adreno-leukodystrophy	1 (2)
Donor type, no. (%)	
Matched related	19 (44)
Matched unrelated	16 (37)
Mismatched related	5 (12)
Mismatched unrelated	3 (7)
Conditioning regimen, no. (%)	
Standard	24 (56)
Reduced intensity	20 (44)
Stem cell source, no. (%)	
Bone marrow	27 (62)
Peripheral blood	14 (33)
Cord blood	2 (5)
cGVHD, no. (%)	
Yes	23 (53)
No	20 (47)
Immunosuppression at the time of analysis, no. (%)	29 (67)
Median time after Allo HSCT for analysis, mo (range)	12 (4-149)

CML/MPD indicates chronic myelogenous leukemia/myeloproliferative disorder; cGVHD, chronic graft-versus-host disease; Allo HSCT, allogeneic hematopoietic stem cell transplantation.

mAb and Flow Cytometric Analysis

An anti-OX40 mAb (131, mouse IgG1) was established in our laboratory [36]. It was used either as a purified protein or it was biotinylated by using EZ-Link® Sulfo-NHS-LC-Biotin (Pierce, Rockford, IL). For flow cytometric analysis, cells were incubated with appropriate concentrations of fluorescein isothiocyanate (FITC)-, phycoerythrin (PE)-, or allophycocyanin (APC)-conjugated mAbs in the dark at 4°C for 20 minutes. The cells were then washed twice and analyzed by flow cytometry on FACSCalibur (BD Biosciences, San Jose, CA) with CELLQuest software (BD Biosciences). PE-conjugated anti-OX40 (PE-anti-OX40), APC-anti-CD45RA, FITC- and PE-anti-interferon γ (IFN-γ), PE-anti-interleukin 4 (IL-4), and Alexa 647-anti-IL7Rα (CD127) were purchased from BD Pharmingen (San Diego, CA). FITC-anti-CD45RO, FITC-anti-CD25, PE-anti-IL-2, FITC-anti-IL-4, and all the isotype-matched control mAbs were obtained from eBioscience (San Diego, CA). FITC-anti-CD62L and FITC-anti-CCR7 were obtained from Beckman Coulter (Fullerton, CA) and R&D systems (Minneapolis, MN), respectively. Intracellular Foxp3 staining was performed by using the PE-conjugated anti-human Foxp3 staining set (PCH101, eBioscience) according to the manufacturer's instructions. Staining of cytoplasmic phosphorylated STAT5 was performed by using Alexa 488-anti-phospho-STAT5 (clone 47, BD Biosciences) according to the manufacturer's instructions. To detect apoptotic cells and dead cells, the cells were stained with 1 μg/mL propidium iodide (PI, Sigma-Aldrich, St. Louis, MO) for 15 minutes at room temperature. For cell proliferation analysis, the cells were labeled for 10 minutes at room temperature with carboxyfluorescein succinimidyl ester (CFSE, Molecular Probes, Eugene, OR) at a final concentration of 5 μM in phosphate-buffered saline (PBS) containing 0.1% bovine serum albumin (BSA, Sigma-Aldrich).

T Cell Isolation and Sorting

Peripheral blood mononuclear cells (PBMC) were isolated from HVs and Allo HSCT recipients by using Ficoll-Hypaque Plus (Amersham Pharmacia Biotech, Piscataway, NJ) density gradient centrifugation. The $CD4^+$ T cells were isolated with CD4 Multisort Kit (Miltenyi Biotec Bergisch Gladbach, Germany) and their purity exceeded 97%. $CD4^+$ T cells were stained with biotinylated anti-OX40 mAb followed by APC-streptavidin (eBioscience) and sorted into $OX40^+$ and $OX40^-$ fractions by FACSAria (BD Biosciences) with FACSDiVA 4.1 software (BD Biosciences). In some experiments, the cells were also stained with PE-anti-CD45RA (BD Pharmingen) and sorted into $OX40^+$ memory ($CD45RA^-OX40^+$) and $OX40^-$ memory ($CD45RA^-OX40^-$) cells. The sorted T cell subsets were more than 90% pure.

Flow Cytometric Analysis of Intracellular Cytokines

For intracellular cytokine staining, cells were suspended in culture medium consisting of RPMI 1640 (Invitrogen, Carlsbad, CA), 10% fetal calf serum (FCS, Hyclone, Logan, UT) and 1% penicillin-streptomycin-glutamine mixture (Invitrogen) and stimulated for 6 or 16 hours in plates coated with anti-CD3 mAb (OKT3, 10 μg/mL) with or without anti-OX40 mAb (131, 10 μg/mL) in the presence of 2 μg/mL soluble anti-CD28 mAb (H046, mouse IgG1, agonistic antibody established in our laboratory; T. Hori, unpublished data) (αCD3/28 or αCD3/28/OX40 stimulation). Brefeldin A (BFA, Sigma-Aldrich) was added at a concentration of 10 μg/mL for the last 4 hours. In some experiments, cells were stimulated with PMA (50 ng/mL, Sigma-Aldrich) and ionomycin (500 ng/mL, Sigma-Aldrich) for 4 hours in the presence of BFA (PMA/Iono stimulation). After stimulation, the cells were washed twice, surface stained with the appropriate mAbs, and fixed with 2% formaldehyde (Wako Pure Chemical Industries, Osaka, Japan) diluted in PBS. The cells were then permeabilized with 0.2% saponin (Sigma-Aldrich)-containing buffer and intracellular cytokine levels were measured by using the relevant mAbs.

Assessment of Cytokine Release by ELISA

To detect IL-2 in the culture supernatants, cells at a concentration of 5×10^5/mL were stimulated for 24 hours with αCD3/28 or αCD3/28/OX40 as described above. The IL-2 levels in the medium were measured by enzyme-linked immunosorbent assay (ELISA) using a rabbit anti-human IL-2 polyclonal Ab (Pierce Biotechnology, Rockford, IL), a biotinylated-anti-human IL-2 mAb (BG5, mouse IgG1, Pierce Biotechnology), and a recombinant human IL-2 standard (Pierce Biotechnology) according to the manufacturer's instructions.

T Cell Culture and Stimulation

For experiments using interleukin 7 (IL-7), cells were suspended in culture medium in the presence or absence of 1 ng/mL IL-7 (Peprotech, Rocky Hill, NJ) for 5 days. For polyclonal stimulation and expansion, isolated $CD4^+$ T cell subsets were suspended in culture medium at a concentration of 5×10^5/mL and stimulated for 12 hours with αCD3/28 or αCD3/28/OX40 in 48- or 96-well plates. The cells were then harvested, washed, and cultured for 4 days in culture medium. In some experiments, after 12 hours of stimulation followed by washing, the cells were cultured in plates coated with anti-OX40

mAb or control mouse IgG1 mAb (eBioscience) for 4 days.

Statistical Analysis

Results are expressed as means ± standard deviation (SD). The statistical significance of differences was determined by using a 2-sided paired *t*-test or Student's *t*-test. Differences with $P < .05$ were considered to be significant.

RESULTS

The CD4$^+$OX40$^+$ T Cell Subset Shares the Characteristics of Central Memory T Cells

We first tested the frequency of OX40-expressing peripheral blood CD4$^+$ T cells in Allo HSCT recipients and HVs by multicolor flowcytometry. Although OX40 is an activation-induced antigen, we found it was expressed on a considerable number of peripheral blood CD4$^+$ T cells from both groups. However, Allo HSCT recipients showed higher frequencies of OX40$^+$ cells (Figure 1A). Further analysis revealed that nearly all of the CD4$^+$OX40$^+$ T cells belonged to the CD45RO$^+$ memory subset and most also expressed CCR7 and CD62L (Figure 1B and C), which indicates that they are central memory T cells. There were no significant differences in the CD4$^+$OX40$^+$ T cells from HVs and Allo HSCT recipients in terms of their CD45RO, CCR7, and CD62L expression. As CD4$^+$CD25$^+$ regulatory T cells are also reported to express OX40 [37-41], we determined the intracellular Foxp3 levels in the CD4$^+$CD25$^+$ T cells and CD4$^+$OX40$^+$ T cells. Although a considerable proportion of the CD4$^+$CD25$^+$ T cells were Foxp3$^+$, fewer than 10% of the CD4$^+$OX40$^+$ T cells from both Allo HSCT recipients and HVs were Foxp3$^+$ (Figure 1D). Recent reports indicated that regulatory T cells have reduced expression of CD127 (IL-7R alpha chain, IL-7Rα) [42]. We also found that the majority of CD4$^+$CD25^{high} T cells were IL-7Rα^{low}. However, CD4$^+$OX40$^+$ T cells were almost all IL-7Rα^{high} (Figure 1D). Collectively, CD4$^+$OX40$^+$ T cells include a minor population of regulatory T cells.

To further characterize the CD4$^+$OX40$^+$ T cells, CD4$^+$ T cells that were freshly isolated from HVs and Allo HSCT recipients were sorted into OX40$^+$ and OX40$^-$ fractions (Figure 2A), stimulated with αCD3/28 for 6 hours, and then subjected to intracellular cytokine staining (Figure 2B and C). There were no differences in the frequency of IL-2-producing cells in the CD4$^+$ T cell population upon αCD3/28 stimulation when CD4$^+$ T cells were isolated with magnetically labeled anti-CD4 mAb or negatively selected to enrich for CD4$^+$ T cells (data not shown). In addition, we confirmed that the binding of anti-OX40 mAb, clone 131, to the cell surface was not enough to affect the IL-2-producing capacity of the cells, because the addition of soluble anti-OX40 mAb to CD4$^+$ T cells did not alter the frequency of IL-2-producing cells after subsequent αCD3/28 stimulation (data not shown). There were marked differences between Allo HSCT recipients and HVs in terms of the cytokine profiles of their OX40$^-$ cells. Although there were very few IL-2-, IFN-γ-, or IL-4-producing cells in the OX40$^-$ cells from HVs, a large proportion (over 30%) of the OX40$^-$ cells from Allo HSCT recipients produced IFN-γ; a small population of these IFN-γ-producing cells (about 5%-10%) also produced IL-2. In contrast, about 10% of the OX40$^+$ cells from both the Allo HSCT recipients and HVs produced IL-2, whereas very few cells produced IFN-γ or IL-4. As we could not detect cells that produce IFN-γ and IL-4 simultaneously (data not shown), we defined the cells that produce IL-2 but not IFN-γ or IL-4 as T_{IL-2} cells. The frequency of T_{IL-2} cells was calculated as follows: (the frequency of all IL-2-producing cells) – (the frequency of IFN-γ- and IL-2-producing cells) – (the frequency of IL-4- and IL-2-producing cells). As shown in Figure 2C, T_{IL-2} cells were only detected in the OX40$^+$ fraction of both Allo HSCT recipients and HVs.

Signaling from IL-7R and Crosslinking of OX40 Robustly Augments IL-2 Production by OX40$^+$ Memory T Cells

As OX40$^+$ cells exclusively exist within the memory cell fraction, we next compared the characteristics of OX40$^+$ memory cells and OX40$^-$ memory cells. To this end, CD4$^+$ T cells of HVs were stained with PE-anti-CD45RA and biotinylated-anti-OX40 Ab before adding streptavidin-APC and sorting them into CD45RA$^-$OX40$^+$ T cells and CD45RA$^-$OX40$^-$ T cells. We regarded the former as OX40$^+$ memory cells and the latter as OX40$^-$ memory cells.

IL-7 is known to be critically involved in maintaining memory CD4$^+$ T cell homeostasis through its ability to induce antigen-independent proliferation in the periphery [43,44]. We found that the addition of IL-7 to culture medium sustained and augmented OX40 expression on CD4$^+$ T cells (data not shown). We then investigated the association between surface expression of OX40 and its ability to produce IL-2. First, freshly sorted OX40$^+$ memory cells were cultured in growth medium unsupplemented with cytokines. Five days later, the cells had lost OX40 expression as well as IL-2-producing capacity in response to αCD3/28 stimulation (the left row of Figure 3A). After sorting and CFSE-labeling, OX40$^+$ memory cells from HVs were then cultured for 5 days in the presence of IL-7. The cells showed enhanced expression of OX40 and an increased frequency of IL-2-producing cells. Meanwhile, culture of OX40$^-$ memory cells with IL-7 neither induced the expression of OX40 nor enhanced the capacity of

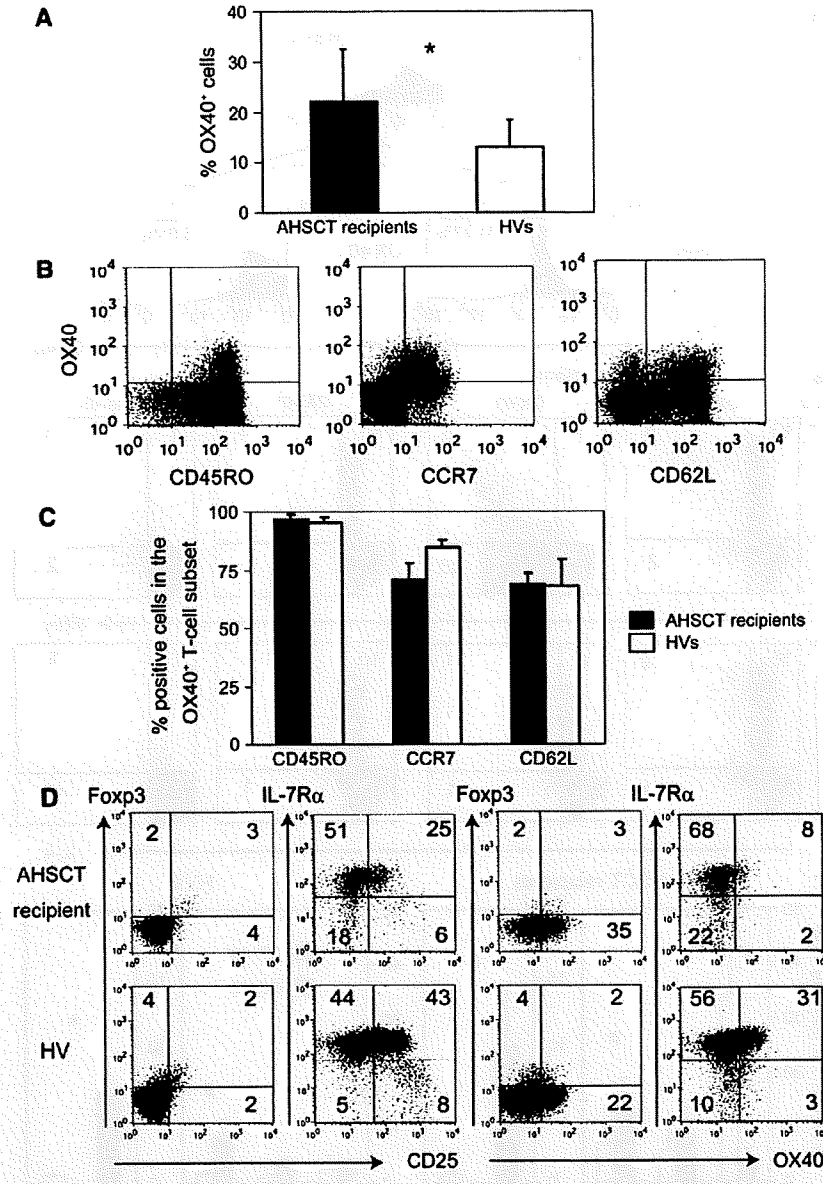

Figure 1. The $CD4^+OX40^+$ T cell subset contains central memory T cells. (A-C) Peripheral blood $CD4^+$ T cells of Allo HSCT recipients and HVs were analyzed for OX40, CD45RO, CCR7, and CD62L expression. (A) The frequencies of OX40-positive cells in the $CD4^+$ T cell subset from 36 Allo HSCT recipients and 13 HVs are shown as means ± SD. $^*P < .01$ (B) The dot plots shown are representative of 25 Allo HSCT recipients. (C) The frequencies of CD45RO-, CCR7-, and CD62L-positive cells in the $OX40^+$ T cell subset from 4 Allo HSCT-recipients and 3 HVs are shown as means ± SD. (D) $CD4^+$ T cells from Allo HSCT recipients and HVs were analyzed for correlations in their expression of CD25, OX40, intracellular Foxp3, and IL-7Rα. The dot plots shown are representative of 6 Allo HSCT recipients (upper) and 3 HVs (lower).

these cells to produce IL-2 (the right row of Figure 3A). Taken together, there seems to be a close association between the expression of OX40 and IL-2-producing capacity. In addition, a significant proportion of $OX40^+$ memory cells treated with IL-7 showed a decreased CFSE staining intensity, indicating that they had begun to proliferate. To determine whether IL-7 differentially delivered signals downstream of IL-7R, the phosphorylation status of cytoplasmic STAT5 was analyzed. As shown in Figure 3B, STAT5 was phosphorylated equally well in $OX40^+$ memory cells and $OX40^-$ memory cells upon IL-7 stimulation.

As previously reported [18], crosslinking of OX40 in addition to αCD3/28 stimulation resulted in a remarkable increase in the amount of IL-2 production by $OX40^+$ memory cells (Figure 4A). When we examined the IL-2 production of $OX40^+$ memory cells at 2-6 and 12-16 hours after stimulation, the costimulation through OX40 increased the frequency of IL-2-producing cells over time from 7% at 2-6 hours to about 13% at 12-16 hours (Figure 4B).

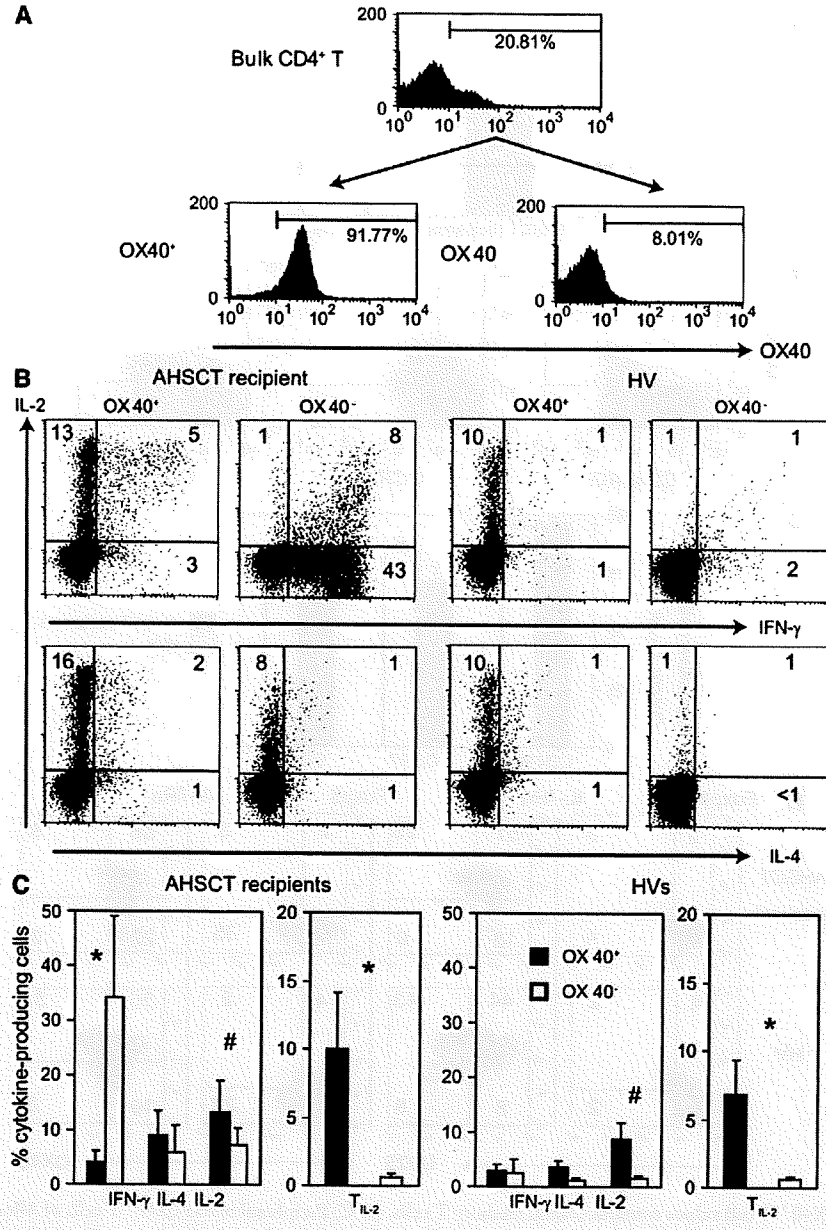

Figure 2. $CD4^+OX40^+$ T cells show an increased propensity to produce IL-2 in response to antigenic stimulation. (A) $CD4^+$ T cells from Allo HSCT recipients and HVs were sorted into $OX40^+$ and $OX40^-$ fractions. (B) Cytokine production by $OX40^+$ and $OX40^-$ cells stimulated with αCD3/28. The data shown are representative of 10 Allo HSCT recipients (left) and 9 HVs (right). (C) The frequencies of cytokine-producing $OX40^+$ and $OX40^-$ cells are shown as means ± SD. T_{IL-2} cells were defined as the cells that produce IL-2 but not IFN-γ or IL-4. $^*P < .01$, $\#P < .05$.

OX40-Mediated Signaling Enhances the Survival and Proliferation of $OX40^+$ Memory T Cells

Having demonstrated that $OX40^+$ memory cells produce massive amounts of IL-2 when the OX40-mediated signal is present during antigenic stimulation, we next examined the effects of OX40-mediated signaling on the survival and proliferation of $OX40^+$ memory cells. For this, sorted $OX40^+$ memory cells from Allo HSCT recipients were labeled with CFSE, stimulated with αCD3/28 or αCD3/28/OX40 for 12 hours, washed, and then cultured for 4 days in growth medium without exogenous cytokines. As a control, $OX40^-$ memory cells were treated similarly. The intensity of the CFSE signal was analyzed to determine the degree to which the cells had proliferated, while their positivity for propidium iodide was analyzed to determine their susceptibility to apoptosis. The $OX40^-$ memory cells of Allo HSCT recipients did not proliferate and lost their viability during the course of cell cultivation (the left row of Figure 5A and B).

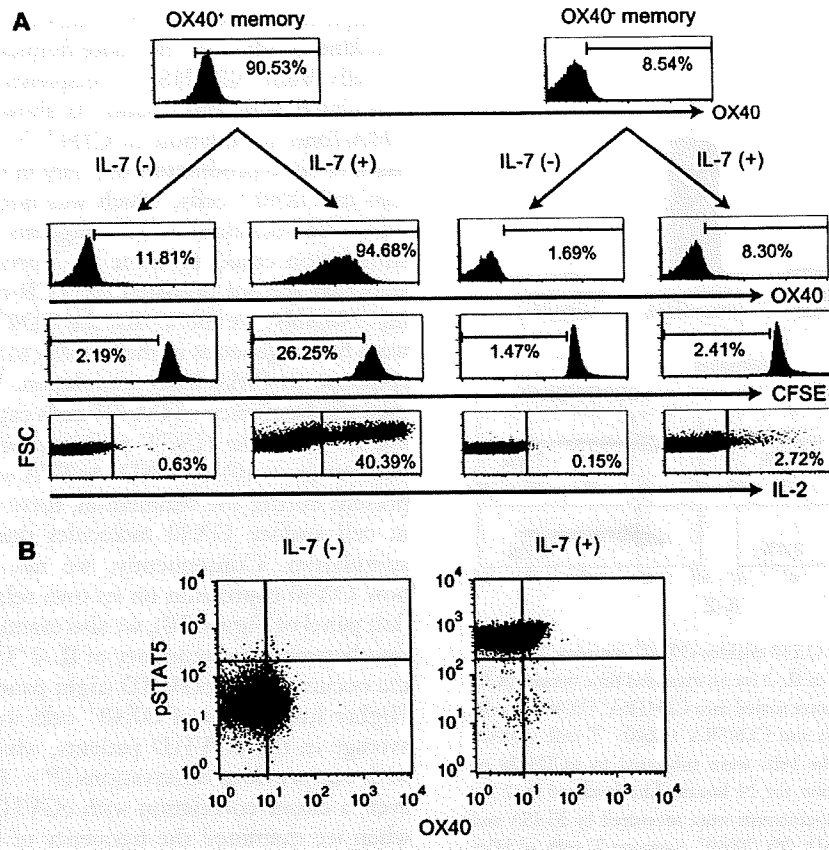

Figure 3. $OX40^+$ memory T cells have greater survival and proliferation potentials. (A) $CD4^+$ T cells from HVs were sorted into $CD45RA^-OX40^+$ T cells ($OX40^+$ memory T cells) and $CD45RA^-OX40^-$ T cells ($OX40^-$ memory T cells). Then, the cells were labeled with CFSE and cultured in the absence or presence of 1 ng/mL IL-7 for 5 days before measuring OX40 expression, division profile, and IL-2-production upon αCD3/28 stimulation. The dot plots shown are representative of 3 independent experiments. (B) $CD4^+$ T cells of HVs were incubated for 15 minutes in the absence or presence of 1 ng/mL IL-7 and analyzed for OX40 and cytoplasmic phosphorylated-STAT5 (pSTAT5). Data are representative of 3 HVs.

In contrast, $OX40^+$ memory cells showed substantial cell growth and high viability in response to αCD3/28 stimulation (the middle row of Figure 5A and B). When OX40 ligation was present during αCD3/28 stimulation, the $OX40^+$ memory cells showed explosive proliferation without impairment of cell viability (the right row of Figure 5A and B).

OX40 is transiently expressed upon TCR triggering, peaking at 48 hours and disappearing after 72 to 96 hours in vitro [19]. We also found that 12-hour stimulation with αCD3/28 induces the expression of OX40 on $OX40^-$ memory cells with similar kinetics. We next evaluated the effect of delivering the OX40-mediated signal after αCD3/28 stimulation (Figure 5C). For this, $OX40^+$ memory and $OX40^-$ memory cells from HVs were labeled with CFSE, and then stimulated with αCD3/28 or αCD3/28/OX40 for 12 hours. After washing, the cells were cultured in plates coated with mouse IgG1 (Figure 5C, upper dot plots and histograms) or anti-OX40 Ab (Figure 5C, lower dot plots and histograms) for an additional 4 days. When the $OX40^+$ memory cells were stimulated with αCD3/28 before incubation with anti-OX40 Ab, a marginal increase in the proportion of CFSE-low and PI-negative cells was seen (the middle row of Figure 5C). As for $OX40^-$ memory cells, despite the acquisition of OX40, they neither showed enhanced proliferation nor increased cell viability when the OX40-mediated signal was subsequently added (the left row of Figure 5C). Thus, for $CD4^+$ T cells to maintain their viability and expand efficiently, antigenic and OX40-mediated signals must be present simultaneously.

Effect of OX40-Mediated Signaling on Differentiation into Effector Memory T Cells

As $CD4^+OX40^+$ T cells are central memory T cells, we next investigated whether OX40-mediated signaling promotes their differentiation into effector memory T cells. For this, $OX40^-$ memory and $OX40^+$ memory cells were stimulated for 12 hours with αCD3/28 or αCD3/28/OX40, washed, cultured in medium without exogenous cytokines for 4 days, and then analyzed for their cytokine profiles. As shown

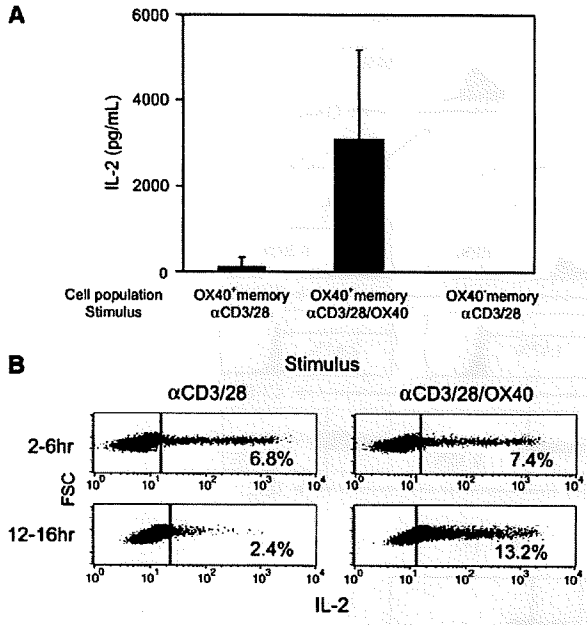

Figure 4. Crosslinking of OX40 enables $OX40^+$ memory T cells to produce massive amounts of IL-2 for an extended time period. (A,B) $CD4^+$ T cells from HVs were sorted into $CD45RA^-OX40^+$ T cells ($OX40^+$ memory T cells) and $CD45RA^-OX40^-$ T cells ($OX40^-$ memory T cells). (A) The cells were subjected to αCD3/28 or αCD3/28/OX40 stimulation for 24 hours. The levels of IL-2 secreted into the culture supernatants were measured by ELISA and are shown as means ± SD. (B) $OX40^+$ memory T cells of HVs were stimulated with αCD3/28 or αCD3/28/OX40 and their IL-2-production 2-6 hours (upper) and 12-16 hours (lower) later was analyzed. The data shown are representative of 3 independent experiments.

in the right row of Figure 6A, the majority of $OX40^+$ memory cells from HVs given αCD3/28/OX40 stimulation did not produce IFN-γ or IL-4. In contrast, the αCD3/28/OX40-stimulated $OX40^+$ memory cells from Allo HSCT recipients showed substantial differentiation into effector memory T cells (the right row of Figure 6B). Interestingly, the directions of polarization differed between the patients: $OX40^+$ memory cells from Case 1, a patient with refractory multiorgan cGVHD, mainly differentiated into the Th1 direction, whereas those from Case 2, a patient with pulmonary cGVHD, differentiated mainly into Th2-type cells. These results suggest that OX40-mediated signaling induces $OX40^+$ memory T cells from Allo HSCT recipients not only to proliferate, but also to differentiate into effector memory T cells.

Allo HSCT Recipients with cGVHD Have Much Higher Frequencies of IL-2-Producing $OX40^+$ Cells among $CD4^+$ T Cells Than Allo HSCT Recipients without cGVHD

As for the detection of intracellular cytokines, PMA/Iono stimulation has been widely used [45]. Compared with αCD3/28 stimulation, we could detect cytokine-producing cells more frequently when $CD4^+$ T cells from Allo HSCT recipients and HVs were stimulated with PMA/Iono. As shown in Figure 7A, PMA/Iono stimulation of $CD4^+$ T cells resulted in massive IL-2 production not only in $OX40^+$ cells but also in $OX40^-$ cells, which was not observed upon αCD3/28 stimulation. This suggests that PMA/Iono stimulation could promote IL-2-production even in cells that are not prepared for TCR-mediated signaling. Notably, we found that the $CD4^+OX40^+$ T cells were heterogeneous in their ability to produce IL-2 in response to PMA/Iono stimulation. We then examined the frequency of $OX40^+$ cells capable of producing IL-2 in Allo HSCT recipients with (n = 15) or without (n = 10) cGVHD. As BFA was continuously present during the stimulation, there was no increase in cell surface OX40 molecules during PMA/Iono stimulation. Consequently, we not only examined how OX40 expression on its own relates to cGVHD (left panel of Figure 7B), we also examined the correlation between the frequency of $IL\text{-}2^+OX40^+$ cells and the occurrence of cGVHD (right panel of Figure 7B). Higher frequencies of $OX40^+$ cells were observed on average in the cGVHD patients, which is consistent with our previous observations ($P = .032$) [33]. However, a closer correlation with cGVHD was detected when we examined the frequency of IL-2-producing $OX40^+$ cells ($P = .007$).

DISCUSSION

Since the concept of central memory and effector memory T cells was proposed [46], the heterogeneity of memory T cells has been an active area of research. Although the origin of central memory and effector memory T cells remains relatively poorly understood [47], it is generally accepted that central memory T cells produce IL-2, show high proliferative potential, and differentiate into cytokine-producing effector cells upon TCR triggering [48]. In this study, we found that circulating $CD4^+OX40^+$ T cells show these characteristics of central memory T cells, and they contain the cells that produce a large amount of IL-2 in response to αCD3/28 stimulation. Not only central memory T cells but also naïve and effector memory T cells have been shown to express OX40 in vivo [49,50]. However, we could not detect OX40 on any circulating naïve and effector memory $CD4^+$ T cells from Allo HSCT recipients or HVs. Although it is unclear why there is preferential expression of OX40 on central memory T cells in the circulating $CD4^+$ T cell population, we speculate as follows: naïve and central memory $CD4^+$ T cells that received activating signals in the lymphoid organs become effector cells or $OX40^+$ "activated" central memory T cells depending on the inflammatory status of the lymphoid tissues.

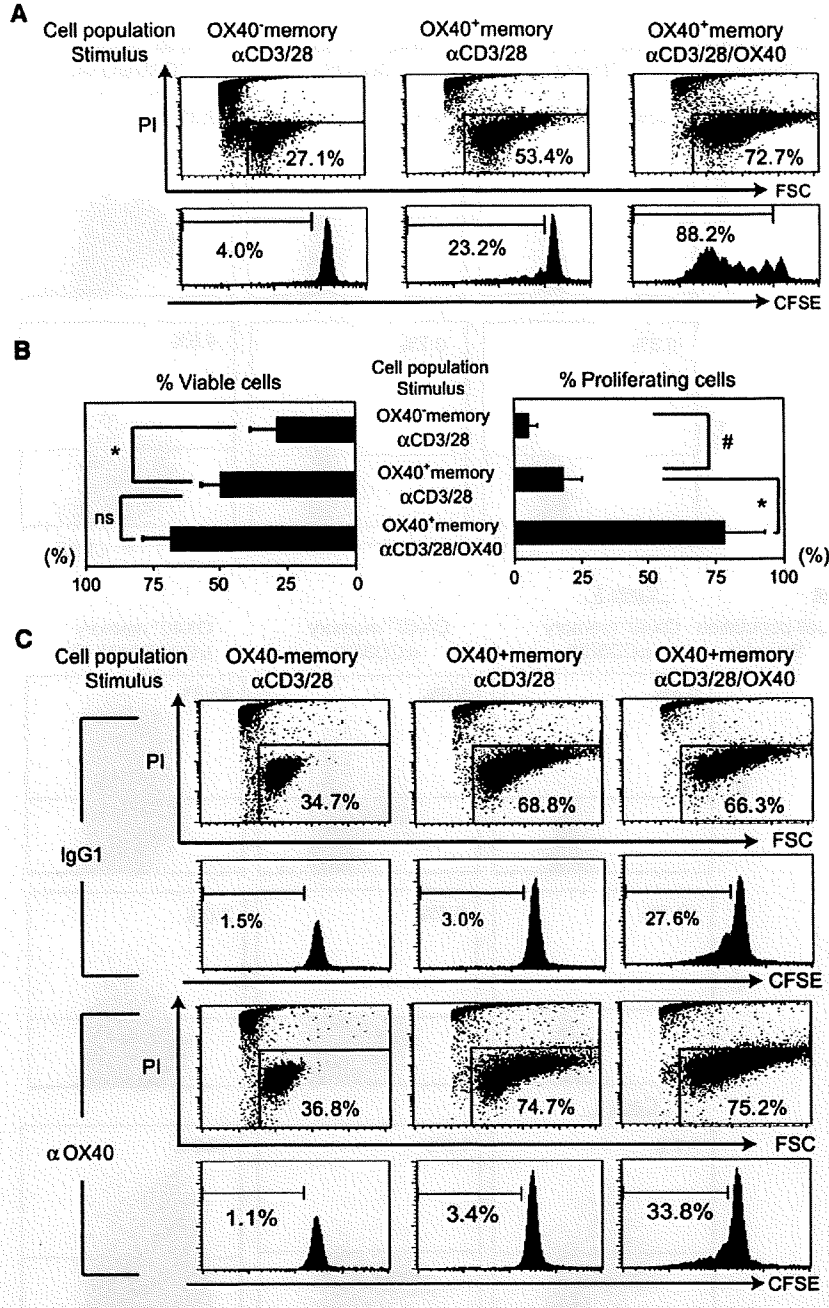

Figure 5. The presence of OX40-mediated signaling during antigenic stimulation results in explosive cell growth. (A,B) $OX40^+$ memory T cells and $OX40^-$ memory T cells from Allo HSCT recipients were labeled with CFSE, stimulated with αCD3/28 or αCD3/28/OX40 for 12 hours, washed, and cultured in growth medium for 4 days. (A) Upper dot plots show the PI-negative cells (viable cells) and lower histograms show the division profile of each cell population. The data shown are representative of 3 experiments. (B) The proportions of viable cells and proliferating cells are shown as means ± SD. $*P < .01$ $\#P < .02$ (C) $OX40^+$ memory T cells and $OX40^-$ memory T cells from HVs were labeled with CFSE, stimulated with αCD3/28 or αCD3/28/OX40 for 12 hours, washed, and then cultured in plates coated with mouse IgG1 (upper dot plots and histograms) or αOX40 Ab (lower dot plots and histograms) for 4 days. Dot plots show the PI staining and histograms show the division profile. The data shown are representative of 3 experiments.

Some of the latter cells return to the circulation as $OX40^+$ central memory T cells. In contrast, effector memory T cells that received antigenic stimulation would not return into circulation because they become effector cells and cannot survive long enough.

Surprisingly, IL-7, a cytokine critically involved in regulating the homeostasis of naïve and memory $CD4^+$ T cells, selectively upregulated the expression of OX40, enhanced IL-2-producing potential, and promoted antigen-independent proliferation in

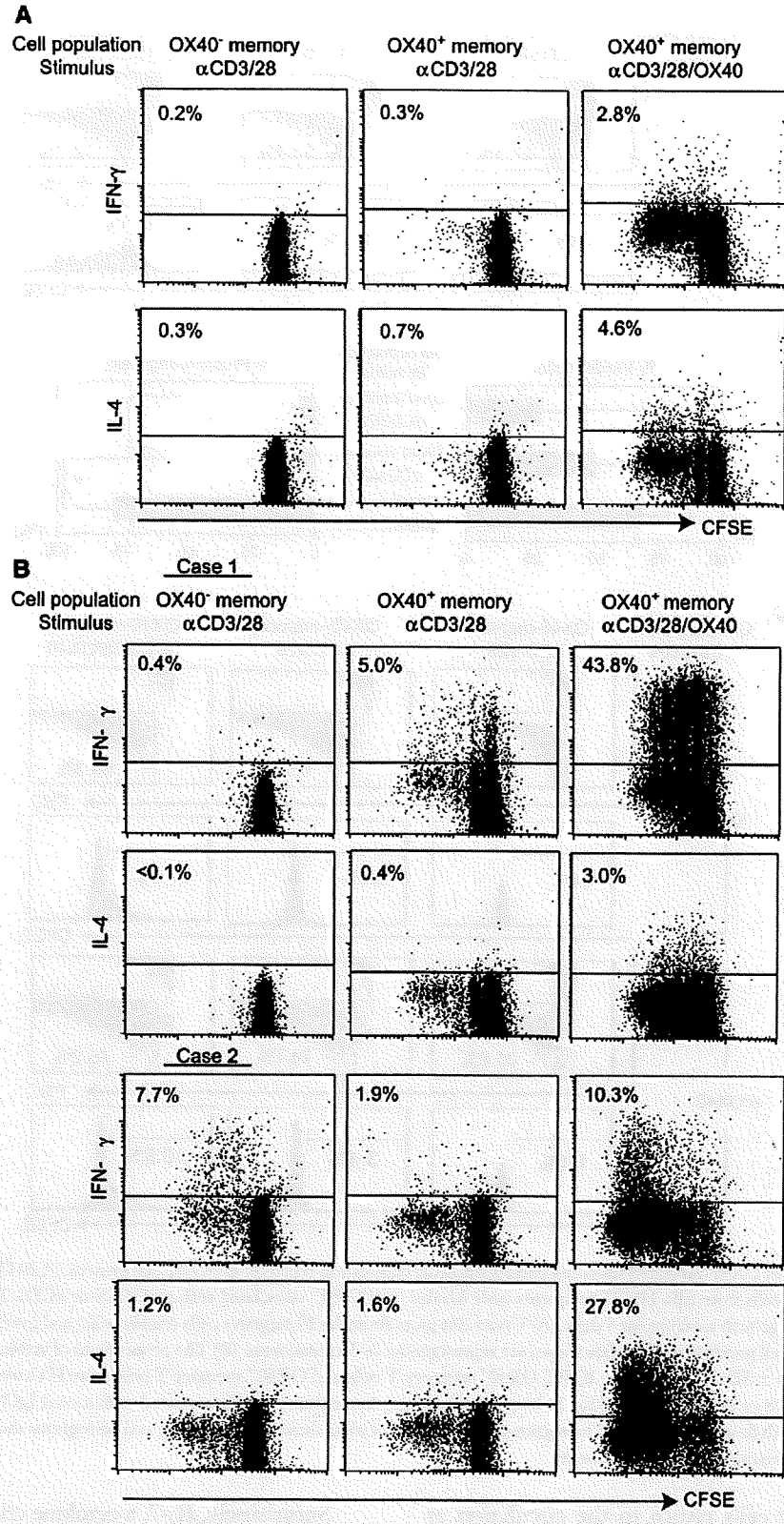

Figure 6. $CD4^+OX40^+$ T cells from Allo HSCT recipients differentiate into Th1 or Th2 effector cells in response to αCD3/28/OX40 stimulation. CFSE-labeled $OX40^+$ memory T cells and $OX40^-$ memory T cells from HVs (A) and Allo HSCT recipients (B) were stimulated with αCD3/28 or αCD3/28/OX40 for 12 hours, washed, cultured in medium for 4 days, and then restimulated with αCD3/28 for 6 hours. The division profile and cytokine production of the cells were then analyzed. (A) The dot plots are representative of 3 HVs. (B) The dot plots are representative of two Allo HSCT recipients.

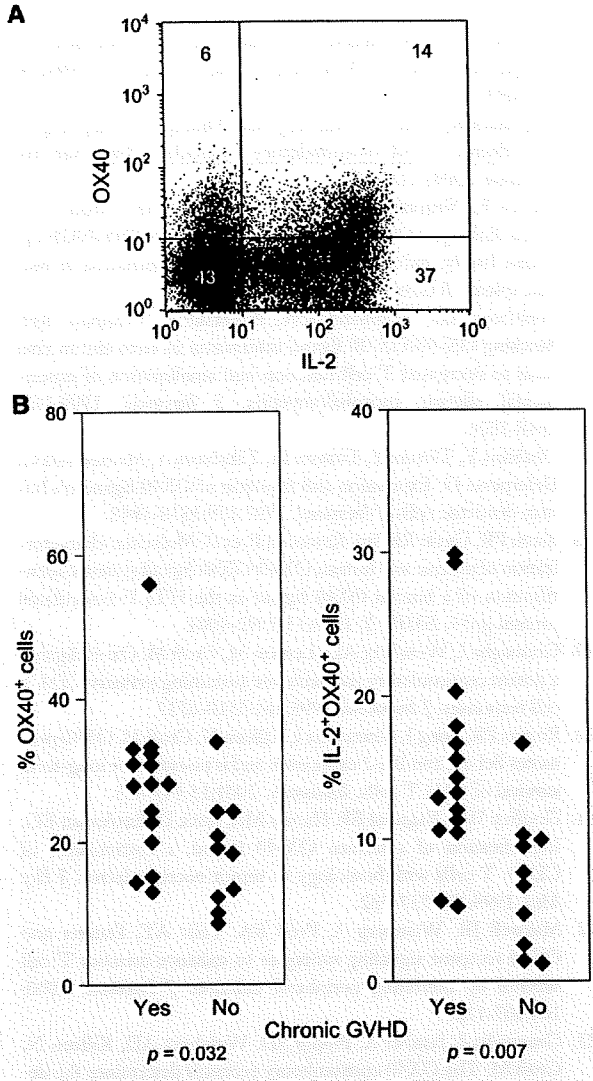

Figure 7. Allo HSCT recipients with cGVHD have much higher frequencies of IL-2-producing $CD4^+OX40^+$ T cells than Allo HSCT recipients without cGVHD. Peripheral blood mononuclear cells from Allo HSCT recipients were stimulated with PMA/Iono stimulation for 4 hours in the continuous presence of BFA. (A) A representative dot plot of surface OX40 and intracellular IL-2 is shown. The gates were set at the $CD4^+$ lymphocytes. (B) Comparison of the frequencies of OX40-expressing and IL-2-producing $OX40^+$ cells in the $CD4^+$ T cell populations of Allo HSCT recipients with (n = 15) and without (n = 10) cGVHD is shown.

$OX40^+$ memory cells. Interestingly, both $OX40^+$ memory and $OX40^-$ memory cells are positive for IL-7Rα, and IL-7 stimulation results in similar levels of STAT5 phosphorylation in both cell subsets. The selective action of IL-7 on $OX40^+$ memory cells implies that IL-7 in $OX40^+$ memory cells invokes a set of transcription factors that is not induced by IL-7 in $OX40^-$ memory cells. In other words, the expression of OX40 in $CD4^+$ T cells may guide IL-7 toward its cellular target. Although IL-7 is known to enhance T cell reconstitution after Allo HSCT [51,52], several reports have raised the concern that exogenous IL-7 administration to Allo HSCT recipients exacerbates GVHD [53,54]. In addition, endogenous IL-7, which is produced by the stromal cells in bone marrow, thymus, and lymph nodes [55], is suspected to ameliorate not only GVHD after Allo HSCT but also the rejection reaction after solid organ transplantation [56,57]. In any case, the significance of the increased sensitivity of $OX40^+$ memory cells to IL-7 will continue to be investigated.

We found that $CD4^+OX40^+$ T cells have a marked potential for proliferation and differentiation in vitro, especially if TCR ligation and costimulation through OX40 are provided simultaneously. Although we previously reported that OX40-mediated signaling on its own activates nuclear factor kappa B through a TNF receptor-associated factor-mediated pathway [58,59], sequential delivery of OX40-mediated signaling after the removal of TCR ligation did not result in cell growth or differentiation at all. Endl et al [60] have suggested that the expression of OX40 in vivo seems to be restricted to $CD4^+$ T cells that are exposed to high-affinity ligands. In addition, it takes at least a day for $CD4^+OX40^-$ memory T cells to express OX40 after antigenic stimulation in vitro. As activated dendritic cells have been shown to express OX40L [17,61], $CD4^+OX40^+$ T cells that enter the secondary lymphoid organs would have great advantage over $CD4^+OX40^-$ T cells in their clonal expansion and differentiation into effector memory T cells after their first encounters with APCs. In this study, there were some differences between $CD4^+OX40^+$ T cells of Allo HSCT recipients and those of HVs. Although $CD4^+OX40^+$ T cells of Allo HSCT recipients explosively proliferated and functionally differentiated in response to αCD3/28/OX40 stimulation, those of HVs did not (Figures 5A, the upper half of Figure 5C, and Figure 6). As the lymphopenic conditions seen in the Allo HSCT recipients promote the production of IL-7 [62], $CD4^+OX40^+$ T cells from Allo HSCT recipients might already have more of the IL-7-mediated signal than the $CD4^+OX40^+$ T cells from HVs before sampling. In addition, it is interesting that $OX40^+$ memory cells of some patients differentiated mainly into Th1-typed cells, whereas others showed Th2-biased differentiation.

Although the $CD4^+OX40^+$ T cell population contains cells that produce a large amount of IL-2, it also includes cells without IL-2-producing capacity. T cells with IL-2-producing capacity have been reported to actively proliferate and differentiate in vivo [63,64]. These results are meaningful when taken together with our finding that the frequency of IL-2-producing $CD4^+OX40^+$ T cells is much higher in Allo HSCT recipients with cGVHD than those without it. Recent studies on murine GVHD models have suggested

that donor-derived alloreactive T cells are activated in secondary lymphoid tissues before they migrate into target organs and cause tissue damage [65,66]. Although further studies are needed, the findings that CD4$^+$OX40$^+$ memory T cells with IL-2-producing capacity have increased sensitivity to IL-7 and can home to lymphoid organs and easily expand and differentiate into effector cells in response to antigenic stimulation, suggesting that they might have a role to play in the process of development and maintenance of cGVHD.

ACKNOWLEDGMENTS

This article was presented as an abstract at the 47th annual meeting of the American Society of Hematology, Atlanta, GA, December 11, 2005. The authors declare that they have no competing financial conflicts.

REFERENCES

1. Lee SJ, Vogelsang G, Flowers ME. Chronic graft-versus-host disease. *Biol Blood Marrow Transplant*. 2003;9:215-233.
2. Shlomchik WD, Couzens MS, Tang CB, et al. Prevention of graft versus host disease by inactivation of host antigen-presenting cells. *Science*. 1999;285:412-415.
3. Higman MA, Vogelsang GB. Chronic graft versus host disease. *Br J Haematol*. 2004;125:435-454.
4. Champlin RE, Passweg JR, Zhang MJ, et al. T-cell depletion of bone marrow transplants for leukemia from donors other than HLA-identical siblings: advantage of T-cell antibodies with narrow specificities. *Blood*. 2000;95:3996-4003.
5. Ho VT, Soiffer RJ. The history and future of T-cell depletion as graft-versus-host disease prophylaxis for allogeneic hematopoietic stem cell transplantation. *Blood*. 2001;98:3192-3204.
6. Mavroudis DA, Dermime S, Molldrem J, et al. Specific depletion of alloreactive T cells in HLA-identical siblings: a method for separating graft-versus-host and graft-versus-leukaemia reactions. *Br J Haematol*. 1998;101:565-570.
7. van Dijk AM, Kessler FL, Stadhouders-Keet SA, Verdonck LF, de Gast GC, Otten HG. Selective depletion of major and minor histocompatibility antigen reactive T cells: towards prevention of acute graft-versus-host disease. *Br J Haematol*. 1999;107:169-175.
8. Andre-Schmutz I, Le Deist F, Hacein-Bey-Abina S, et al. Immune reconstitution without graft-versus-host disease after haemopoietic stem-cell transplantation: a phase 1/2 study. *Lancet*. 2002;360:130-137.
9. Perreault C, Decary F, Brochu S, Gyger M, Belanger R, Roy D. Minor histocompatibility antigens. *Blood*. 1990;76:1269-1280.
10. Vogelsang GB. How I treat chronic graft-versus-host disease. *Blood*. 2001;97:1196-1201.
11. Pavletic SZ, Carter SL, Kernan NA, et al. Influence of T-cell depletion on chronic graft-versus-host disease: results of a multicenter randomized trial in unrelated marrow donor transplantation. *Blood*. 2005;106:3308-3313.
12. Sakoda Y, Hashimoto D, Asakura S, et al. Donor-derived thymic-dependent T cells cause chronic graft-versus-host disease. *Blood*. 2007;109:1756-1764.
13. Latza U, Durkop H, Schnittger S, et al. The human OX40 homolog: cDNA structure, expression and chromosomal assignment of the ACT35 antigen. *Eur J Immunol*. 1994;24:677-683.
14. Sugamura K, Ishii N, Weinberg AD. Therapeutic targeting of the effector T-cell co-stimulatory molecule OX40. *Nat Rev Immunol*. 2004;4:420-431.
15. Stuber E, Neurath M, Calderhead D, Fell HP, Strober W. Cross-linking of OX40 ligand, a member of the TNF/NGF cytokine family, induces proliferation and differentiation in murine splenic B cells. *Immunity*. 1995;2:507-521.
16. Weinberg AD, Wegmann KW, Funatake C, Whitham RH. Blocking OX-40/OX-40 ligand interaction in vitro and in vivo leads to decreased T cell function and amelioration of experimental allergic encephalomyelitis. *J Immunol*. 1999;162:1818-1826.
17. Ohshima Y, Tanaka Y, Tozawa H, Takahashi Y, Maliszewski C, Delespesse G. Expression and function of OX40 ligand on human dendritic cells. *J Immunol*. 1997;159:3838-3848.
18. Baum PR, Gayle RB 3rd, Ramsdell F, et al. Molecular characterization of murine and human OX40/OX40 ligand systems: identification of a human OX40 ligand as the HTLV-1-regulated protein gp34. *EMBO J*. 1994;13:3992-4001.
19. Gramaglia I, Weinberg AD, Lemon M, Croft M. Ox-40 ligand: a potent costimulatory molecule for sustaining primary CD4 T cell responses. *J Immunol*. 1998;161:6510-6517.
20. Rogers PR, Song J, Gramaglia I, Killeen N, Croft M. OX40 promotes Bcl-xL and Bcl-2 expression and is essential for long-term survival of CD4 T cells. *Immunity*. 2001;15:445-455.
21. Godfrey WR, Fagnoni FF, Harara MA, Buck D, Engleman EG. Identification of a human OX-40 ligand, a costimulator of CD4+ T cells with homology to tumor necrosis factor. *J Exp Med*. 1994;180:757-762.
22. Maxwell JR, Weinberg A, Prell RA, Vella AT. Danger and OX40 receptor signaling synergize to enhance memory T cell survival by inhibiting peripheral deletion. *J Immunol*. 2000;164:107-112.
23. Gramaglia I, Jember A, Pippig SD, Weinberg AD, Killeen N, Croft M. The OX40 costimulatory receptor determines the development of CD4 memory by regulating primary clonal expansion. *J Immunol*. 2000;165:3043-3050.
24. Jember AG, Zuberi R, Liu FT, Croft M. Development of allergic inflammation in a murine model of asthma is dependent on the costimulatory receptor OX40. *J Exp Mede*. 2001;193:387-392.
25. Weinberg AD, Bourdette DN, Sullivan TJ, et al. Selective depletion of myelin-reactive T cells with the anti-OX-40 antibody ameliorates autoimmune encephalomyelitis. *Nat Med*. 1996;2:183-189.
26. Yoshioka T, Nakajima A, Akiba H, et al. Contribution of OX40/OX40 ligand interaction to the pathogenesis of rheumatoid arthritis. *Eur J Immunol*. 2000;30:2815-2823.
27. Salek-Ardakani S, Song J, Halteman BS, et al. OX40 (CD134) controls memory T helper 2 cells that drive lung inflammation. *J Exp Med*. 2003;198:315-324.
28. Higgins LM, McDonald SA, Whittle N, Crockett N, Shields JG, MacDonald TT. Regulation of T cell activation in vitro and in vivo by targeting the OX40-OX40 ligand interaction: amelioration of ongoing inflammatory bowel disease with an OX40-IgG fusion protein, but not with an OX40 ligand-IgG fusion protein. *J Immunol*. 1999;162:486-493.

29. Tsukada N, Akiba H, Kobata T, Aizawa Y, Yagita H, Okumura K. Blockade of CD134 (OX40)-CD134L interaction ameliorates lethal acute graft-versus-host disease in a murine model of allogeneic bone marrow transplantation. *Blood.* 2000; 95:2434-2439.
30. Blazar BR, Sharpe AH, Chen AI, et al. Ligation of OX40 (CD134) regulates graft-versus-host disease (GVHD) and graft rejection in allogeneic bone marrow transplant recipients. *Blood.* 2003;101:3741-3748.
31. Buenafe AC, Weinberg AD, Culbertson NE, Vandenbark AA, Offner H. V beta CDR3 motifs associated with BP recognition are enriched in OX-40+ spinal cord T cells of Lewis rats with EAE. *J Neurosci Res.* 1996;44:562-567.
32. Tittle TV, Weinberg AD, Steinkeler CN, Maziarz RT. Expression of the T-cell activation antigen, OX-40, identifies alloreactive T cells in acute graft-versus-host disease. *Blood.* 1997;89: 4652-4658.
33. Kotani A, Ishikawa T, Matsumura Y, et al. Correlation of peripheral blood OX40+(CD134+) T cells with chronic graft-versus-host disease in patients who underwent allogeneic hematopoietic stem cell transplantation. *Blood.* 2001;98:3162-3164.
34. Hitomi T, Mezaki T, Tsujii T, et al. Improvement of central motor conduction after bone marrow transplantation in adrenoleukodystrophy. *J Neurol Neurosurg Psychiatry.* 2003;74: 373-375.
35. Shulman HM, Sullivan KM, Weiden PL, et al. Chronic graft-versus-host syndrome in man. A long-term clinicopathologic study of 20 Seattle patients. *Am J Med.* 1980;69:204-217.
36. Imura A, Hori T, Imada K, et al. The human OX40/gp34 system directly mediates adhesion of activated T cells to vascular endothelial cells. *J Exp Med.* 1996;183:2185-2195.
37. Gavin MA, Clarke SR, Negrou E, Gallegos A, Rudensky A. Homeostasis and anergy of CD4(+)CD25(+) suppressor T cells in vivo. *Nat Immunol.* 2002;3:33-41.
38. McHugh RS, Whitters MJ, Piccirillo CA, et al. CD4(+)CD25(+) immunoregulatory T cells: gene expression analysis reveals a functional role for the glucocorticoid-induced TNF receptor. *Immunity.* 2002;16:311-323.
39. Takeda I, Ine S, Killeen N, et al. Distinct roles for the OX40-OX40 ligand interaction in regulatory and nonregulatory T cells. *J Immunol.* 2004;172:3580-3589.
40. Valzasina B, Guiducci C, Dislich H, Killeen N, Weinberg AD, Colombo MP. Triggering of OX40 (CD134) on CD4(+)CD25+ T cells blocks their inhibitory activity: a novel regulatory role for OX40 and its comparison with GITR. *Blood.* 2005;105:2845-2851.
41. Streeter PR, Zhang X, Tittle TV, Schon CN, Weinberg AD, Maziarz RT. CD25 expression distinguishes functionally distinct alloreactive CD4 CD134 (OX40) T-cell subsets in acute graft-versus-host disease. *Biol Blood Marrow Transplant.* 2004; 10:298-309.
42. Seddiki N, Santner-Nanan B, Martinson J, et al. Expression of interleukin (IL)-2 and IL-7 receptors discriminates between human regulatory and activated T cells. *J Exp Med.* 2006;203: 1693-1700.
43. Fry TJ, Mackall CL. Interleukin-7: from bench to clinic. *Blood.* 2002;99:3892-3904.
44. Surh CD, Boyman O, Purton JF, Sprent J. Homeostasis of memory T cells. *Immunol Rev.* 2006;211:154-163.
45. Jung T, Schauer U, Heusser C, Neumann C, Rieger C. Detection of intracellular cytokines by flowcytometry. *J Immunol Methods.* 1993;159:197-207.
46. Sallusto F, Lenig D, Forster R, Lipp M, Lanzavecchia A. Two subsets of memory T lymphocytes with distinct homing potentials and effector functions. *Nature.* 1999;401: 708-712.
47. Lanzavecchia A, Sallusto F. Progressive differentiation and selection of the fittest in the immune response. *Nat Rev Immunol.* 2002;2:982-987.
48. Sallusto F, Geginat J, Lanzavecchia A. Central memory and effector memory T cell subsets: function, generation, and maintenance. *Annu Rev Immunol.* 2004;22:745-763.
49. Stuber E, Strober W. The T cell-B cell interaction via OX40-OX40L is necessary for the T cell-dependent humoral immune response. *J Exp Med.* 1996;183:979-989.
50. Kotani A, Hori T, Fujita T, et al. Involvement of OX40 ligand(+) mast cells in chronic GVHD after allogeneic hematopoietic stem cell transplantation. *Bone Marrow Transplant.* 2007.
51. Alpdogan O, Schmaltz C, Muriglan SJ, et al. Administration of interleukin-7 after allogeneic bone marrow transplantation improves immune reconstitution without aggravating graft-versus-host disease. *Blood.* 2001;98:2256-2265.
52. Bolotin E, Smogorzewska M, Smith S, Widmer M, Weinberg K. Enhancement of thymopoiesis after bone marrow transplant by in vivo interleukin-7. *Blood.* 1996;88:1887-1894.
53. Gendelman M, Hecht T, Logan B, Vodanovic-Jankovic S, Komorowski R, Drobyski WR. Host conditioning is a primary determinant in modulating the effect of IL-7 on murine graft-versus-host disease. *J Immunol.* 2004;172: 3328-3336.
54. Sinha ML, Fry TJ, Fowler DH, Miller G, Mackall CL. Interleukin 7 worsens graft-versus-host disease. *Blood.* 2002;100: 2642-2649.
55. Napolitano LA, Grand RM, Deeks SG, et al. Increased production of IL-7 accompanies HIV-1-mediated T-cell depletion: implication for T-cell homeostasis. *Nat Med.* 2001;7:73-79.
56. Chung B, Dupl EP, Min D, Barsky L, Smiley N, Weinberg KI. Prevention of graft-versus-host disease by anti-IL-7Ralpha antibody. *Blood.* 2007;110:2803-2810.
57. Codarri L, Vallotton L, Ciuffreda D, et al. Expansion and tissue infiltration of an allospecific CD4+CD25+CD45RO+IL-7Ralphahigh cell population in solid organ transplant recipients. *J Exp Med.* 2007;204:1533-1541.
58. Kawamata S, Hori T, Imura A, Takaori-Kondo A, Uchiyama T. Activation of OX40 signal transduction pathways leads to tumor necrosis factor receptor-associated factor (TRAF) 2- and TRAF5-mediated NF-kappaB activation. *J Biol Chem.* 1998; 273:5808-5814.
59. Takaori-Kondo A, Hori T, Fukunaga K, Morita R, Kawamata S, Uchiyama T. Both amino- and carboxyl-terminal domains of TRAF3 negatively regulate NF-kappaB activation induced by OX40 signaling. *Biochem Biophys Res Commun.* 2000;272: 856-863.
60. Endl J, Rosinger S, Schwarz B, et al. Coexpression of CD25 and OX40 (CD134) receptors delineates autoreactive T-cells in type 1 diabetes. *Diabetes.* 2006;55:50-60.
61. Ito T, Wang YH, Duramad O, et al. TSLP-activated dendritic cells induce an inflammatory T helper type 2 cell response through OX40 ligand. *J Exp Med.* 2005;202:1213-1223.
62. Bolotin E, Annett G, Parkman G, Weinberg K. Serum levels of IL-7 in bone marrow transplant recipients: relationship to clinical characteristics and lymphocyte count. *Bone Marrow Transplant.* 1999;23:783-788.

63. Saparov A, Wagner FH, Zheng R, et al. Interleukin-2 expression by a subpopulation of primary T cells is linked to enhanced memory/effector function. *Immunity*. 1999;11:271-280.
64. Dooms H, Kahn E, Knoechel B, Abbas AK. IL-2 induces a competitive survival advantage in T lymphocytes. *J Immunol*. 2004; 172:5973-5979.
65. Wysocki CA, Panoskaltsis-Mortari A, Blazar BR, Serody JS. Leukocyte migration and graft-versus-host disease. *Blood*. 2005;105:4191-4199.
66. Beilhack A, Schulz S, Baker J, et al. In vivo analyses of early events in acute graft-versus-host disease reveal sequential infiltration of T-cell subsets. *Blood*. 2005;106:1113-1122.

Kpm/Lats2 is linked to chemosensitivity of leukemic cells through the stabilization of p73

Masahiro Kawahara,[1] Toshiyuki Hori,[1] Kazuhisa Chonabayashi,[1] Tsutomu Oka,[2] Marius Sudol,[2,3] and Takashi Uchiyama[1]

[1]Department of Hematology and Oncology, Graduate School of Medicine, Kyoto University, Kyoto, Japan; [2]Laboratory of Signal Transduction and Proteomic Profiling, Weis Center for Research, Danville, PA; and [3]Department of Medicine, Mount Sinai School of Medicine, New York, NY

Down-regulation of the Kpm/Lats2 tumor suppressor is observed in various malignancies and associated with poor prognosis in acute lymphoblastic leukemia. We documented that Kpm/Lats2 was markedly decreased in several leukemias that were highly resistant to conventional chemotherapy. Silencing of Kpm/Lats2 expression in leukemic cells did not change the rate of cell growth but rendered the cells more resistant to DNA damage–inducing agents. Expression of p21 and PUMA was strongly induced by these agents in control cells, despite defective p53, but was only slightly induced in Kpm/Lats2-knockdown cells. DNA damage–induced nuclear accumulation of p73 was clearly observed in control cells but hardly detected in Kpm/Lats2-knockdown cells. Chromatin immunoprecipitation (ChIP) assay showed that p73 was recruited to the *PUMA* gene promoter in control cells but not in Kpm/Lats2-knockdown cells after DNA damage. The analyses with transient coexpression of Kpm/Lats2, YAP2, and p73 showed that Kpm/Lats2 contributed the stability of YAP2 and p73, which was dependent on the kinase function of Kpm/Lats2 and YAP2 phosphorylation at serine 127. Our results suggest that Kpm/Lats2 is involved in the fate of p73 through the phosphorylation of YAP2 by Kpm/Lats2 and the induction of p73 target genes that underlie chemosensitivity of leukemic cells. (Blood. 2008;112:3856-3866)

Introduction

The *Warts* (*Wts*) tumor suppressor gene (also termed *Lats* after large tumor suppressor) was first identified by mitotic recombination of somatic cells and screening for homozygous mutants with overproliferation phenotype in *Drosophila melanogaster*.[1,2] This discovery initiated a series of genetic studies in *Drosophila* that led to the delineation of a new signaling network named the Hippo pathway, which is now known to regulate cell growth, cell survival, and organ size in developing animals.[3-5] This pathway consists of a kinase cascade in its core where Hippo (Hpo) phosphorylates and activates Wts/Lats,[6] which then in turn phosphorylates and inactivates Yorkie (Yki), a transcription coactivator. Inactivation of Yki results in control of cell survival and cell growth through down-regulation of *Drosophila* inhibitor of apoptosis 1 (Diap1) and Cyclin E.[7] Salvador (Sav),[8,9] a scaffold protein for Hpo, and Mats (mob as tumor suppressor),[10-12] a partner and potentiater of Wts, are also essential components of this pathway. Furthermore, recent evidence has placed Expanded (EX), Merlin (Mer),[13] both 4.1 family proteins, and Fat (FT),[14-17] the atypical cadherin, in the upstream of the Hippo pathway although their connection to the kinase cascade is largely based on genetic epitasis. The Hippo pathway is believed to be conserved throughout species because some of the mammalian homologues have been shown to compensate the corresponding defects in the *Drosophila* Hippo pathway. At present, however, only a small part of the mammalian Hippo pathway has been experimentally substantiated.

Kpm (alternatively named Lats2) is one of the 2 human homologues of *Drosophila Wts*.[18,19] In parallel to *Drosophila Wts*, we and others have shown the critical involvement of *Kpm*/Lats2 in regulation of cell growth and survival. Kpm/Lats2 overexpression results in the cell cycle arrest in G2/M phase via inhibition of Cdc2–Cyclin B kinase activity leading eventually to apoptosis,[20] inhibition of G1/S transition via down-regulation of Cyclin E/Cdk2 kinase activity,[21] or apoptosis via down-regulation of Bcl-2 and Bcl-xL.[22] Kpm/Lats2 binds to Mdm2 and inhibits its E3 ubiquitin ligase activity, resulting in the stabilization of p53 and leading to the p53-dependent G1/S arrest in nocodazole-treated cells.[23] Moreover, Kpm/Lats2 is a target gene of p53 both in mammalian as well as in *Drosophila* cells,[24,25] suggesting that Kpm/Lats2 may be a positive-feedback-loop regulator of p53. Kpm/Lats2 knockout mice are embryonically lethal and fibroblasts isolated from these mice appear to be defective in contact inhibition and display genomic instability through multipolar mitotic spindles.[26,27] Mst-2, one of the mammalian orthologues of *Drosophila* Hippo, has been reported to phosphorylate Kpm/Lats2 as well as its related kinase, Lats1.[28] However, the downstream function of Kpm/Lats2 has not been elucidated in the Hippo pathway in mammals, because the interaction between Kpm/Lats2 and Yes-associated protein (YAP), the mammalian orthologue of Yki, has not been shown.

Yes-kinase associated protein (YAP) was initially isolated by virtue of its binding to the Src family member, a nonreceptor tyrosine kinase Yes.[29,30] The cloning of YAP revealed a new modular protein domain, known today as the WW domain, which recognizes a specific set of proline-rich ligands. The YAP gene encodes at least 2 isoforms: YAP1 and YAP2, which are generated by differential splicing and differ in the number of WW domains they contain. YAP1 has one WW domain and YAP2 has 2 WW domains.[30,31] In human epithelial cells, YAP plays a potentially oncogenic role through several signaling interactions with potent

Submitted September 12, 2007; accepted April 19, 2008. Prepublished online as *Blood* First Edition paper, June 18, 2008; DOI 10.1182/blood-2007-09-111773.

The online version of this article contains a data supplement.

The publication costs of this article were defrayed in part by page charge payment. Therefore, and solely to indicate this fact, this article is hereby marked "advertisement" in accordance with 18 USC section 1734.

© 2008 by The American Society of Hematology

signaling proteins.[32-36] Furthermore, a region of human chromosome 11 at position q22 has been reported to be frequently amplified in various cancers, and this amplicon contains *YAP* and *cIAP2* loci.[37,38] Curiously, YAP has also been shown to regulate apoptosis. For example, YAP forms a signaling complex with p53-binding protein-2, a known regulator of the apoptotic activity of p53.[39,40] YAP interacts with and coactivates p73 to induce transcription of its target genes, leading to apoptosis and cell cycle arrest.[41] In sum, YAP has a capacity to function either as an oncogene or as a proapoptotic factor.

Recent clinical studies have indicated that the expression level of Kpm/Lats2 correlates with clinical course of some malignancies. Down-regulation of Kpm/Lats2 was associated with larger tumor size and high number of metastatic lymph nodes in breast cancers,[42] and it was significantly associated with poor prognosis in acute lymphoblastic leukemia (ALL).[43] The relative level of Kpm/Lats2 expression was shown with high confidence as the most important prognostic factor in predicting disease-free survival in ALL, even compared with the *BCR-ABL* gene fusion, which is so far the most significant factor for poor prognosis. However, the molecular and cellular mechanisms underlying the poor clinical course in leukemias that have a relatively low level of Kpm/Lats2 expression have not been investigated in detail.

In the present study, we documented that Kpm/Lats2 was down-regulated also in adult T-cell leukemia (ATL) and natural killer (NK) leukemia/lymphoma, both of which are known to be highly resistant to conventional chemotherapy. Then we addressed the molecular mechanism underlying the chemoresistance associated with low Kpm/Lats2 expression. We herewith report that down-regulation of Kpm/Lats2 leads to chemoresistance through insufficient nuclear accumulation of p73, resulting in poor induction of its target genes p21 and p53 up-regulated modulator of apoptosis (PUMA).

Methods

Cells and cell culture

Leukemic cell lines including KG-1a[44] were cultured in 10% heat-inactivated fetal bovine serum (FBS; Invitrogen, Paisley, United Kingdom) containing Iscove modified Dulbecco medium (IMDM; Invitrogen) with 2 mM L-glutamine and antibiotics (Invitrogen), and only ED-40515^{+}[45] was cultured in the same medium with 100 IU/mL recombinant human interleukin-2 (rhIL-2; Shionogi, Osaka, Japan). Adherent cell lines including 293T, GP2-293, and HeLa were cultured using Dulbecco modified Eagle medium (DMEM; Invitrogen) instead of IMDM. All cells were maintained at 37°C in a 5% CO_2 humidified incubator. Clinical samples from patients with leukemia were cryopreserved in our laboratory as described previously.[46-48] Normal peripheral mononuclear cells (PBMCs) were purified from healthy donor with informed consent; normal CD4^{+} T cells and normal CD56^{+} cells were purified using magnetic-activated cell sorting (MACS) CD4^{+} T-cell isolation kit (Miltenyi Biotec, Bergisch Gladbach, Germany) and MACS CD56^{+} isolation kit (Miltenyi Biotec), respectively. All the clinical samples were taken with informed consent and used only for in vitro study following the guideline of the institutional review board of Kyoto University. This study was conducted in accordance with the Declaration of Helsinki.

Isolation of total RNA and quantitative real-time PCR

The isolation of total RNA was performed using RNeasy Mini kit (Qiagen, Valencia, CA). The cDNA was synthesized from 1 μg total RNA by ImProm-II Reverse Transcription system (Promega, Madison, WI). Quantitative real-time polymerase chain reaction (PCR) was analyzed using SYBR Green (Invitrogen) on an ABI Prism 7900HT instrument (Applied Biosystems, Foster City, CA). More than one internal control was always used in each analysis, and only when relative amounts of internal controls were constant for each sample, were data considered valid. The list of gene-specific primers is provided in Table 1.

Table 1. Primer sequence for real-time PCR or semiquantitative RT-PCR

Gene	Primer sequence
Kpm (for RT-PCR)	
Forward	GCTGACTTTGGCCATTGAGAGTGTC
Reverse	CATCTACGGGGTCGAAATTCGAGGT
Kpm (for real-time)	
Forward	GTTCAGGTGGACTCACAATTCC
Reverse	CGACAGTTAGACACATCATCCCA
Lats1	
Forward	TGGTCATATTAAATTGACTGAC
Reverse	CCACATCGACAGCTTGAGGG
YAP	
Forward	TGGGAGATGGCAAAGACATCTTCTG
Reverse	ACACTGGATTTTGAGTCCCACCATC
cIAP1	
Forward	CAGCCTGAGCAGCTTGCAA
Reverse	CAAGCCACCATCACAACAAAA
cIAP2	
Forward	TCCGTCAAGTTCAAGCCAGTT
Reverse	TCTCCTGGGCTGTCTGATGTG
survivin	
Forward	TGCCTGGCAGCCCTTTC
Reverse	CCTCCAAGAAGGGCCAGTTC
XIAP	
Forward	AGTGGTAGTCCTGTTTCAGCATCA
Reverse	CCGCACGGTATCTCCTTCA
bcl-2	
Forward	AGGAAGTGAACATTTCGGTGAC
Reverse	GCTCAGTTCCAGGACCAGG
p21	
Forward	CTGTCACTGTCTTGTACCCT
Reverse	GGTAGAAATCTGTCATGCTGC
PUMA	
Forward	GACCTCAACGCACAGTA
Reverse	CTAATTGGGCTCCATCT
TAp73	
Forward	GCACCACGTTTGAGCACCTCT
Reverse	GCAGATTGAACTGGGCCATGA
β-actin	
Forward	TCCTGTGGCATCCACGAAACT
Reverse	GAAGCATTTGCGGTGGACGAT
hprt	
Forward	TGACACTGGCAAAACAATGCA
Reverse	GGTCCTTTTCACCAGCAAGCT
gapdh	
Forward	GAAGGTGAAGGTCGGAGTC
Reverse	GAAGATGGTGATGGGATTTC

Plasmids

The plasmids for expression of HA-tagged Kpm wild-type (wt) form and Kpm-kinase dead (kd) form (mutant form K697 to A) were described before.[18] FLAG-tagged YAP1, YAP1-S127A (mutant form S127 to A; S127 is Akt-phosphorylation site), YAP1-WW* (mutant form of WW domain), YAP2, YAP2-S127A, YAP2-1WW* (mutant form of first WW domain), and YAP2-2WW* (mutant form of second WW domain) inserted into pFLAG-CMV2 vector were described previously 33. TAp73α inserted into pcDNA3 vector, described elsewhere,[49] was a gift of Dr Yoshihide Ueda (Kyoto University). The plasmid expressing Kpm/Lats2 shRNA was generated by insertion of target sequence (loop sequence, CTGTGAAGC-CACAGATGGG) and target antisense sequence into the retrovirus (RV)

vector, pSINsi-hU6 (Takara, Kusatsu, Japan). Kpm/Lats2 target sequence is TTCACCTTCCGAAGGTTCT; control sequence is TCGTACTCTCGTCTTCGAT. Control sequence was constructed by shuffling Kpm/Lats2 target sequence, and it was confirmed using BLASTN that control sequence did not target any other genes.[50] p73 target sequence is GGATTCCAGCATGGACGTCTT, as described elsewhere.[51] pVSV-G was used as the envelope plasmid.

Plasmid transfection and retrovirus vector transduction

Plasmids were transfected into 293T cells using CalPhos mammalian transfection kit (Clontech, Mountain View, CA) or FuGENE-HD (Roche, Basel, Switzerland) for coimmunoprecipitation assays. Retroviruses were generated by cotransfection of shRNA containing retrovirus vector and pVSV-G into GP2-293 packaging cells with CalPhos kit and collected by ultracentrifugation. Retronectin (Takara) was used to transduce leukemic cells with retroviruses. After transduction, pools of cells in bulk selected with 0.5 mg/mL G-418 (Nacalai Tesque, Kyoto, Japan) were used in the following assays.

MTT assay

To evaluate cell viability, an appropriate number of cells were seeded with doxorubicin (DXR; Pharmacia, Milan, Italy) or etoposide (ETP; Bristol-Myers, New York, NY) in appropriate concentrations. Next MTT assays were performed using WST-8 (Nacalai Tesque) according to the manufacturer's protocol and analyzed with microplate reader Benchmark (Bio-Rad, Hercules, CA) as described previously.[20]

Antibodies, immunoprecipitation, and Western blotting

The following antibodies were purchased or prepared in our laboratory: anti-FLAG mouse monoclonal antibody (Sigma-Aldrich, St Louis, MO), anti-HA mouse monoclonal antibody (Roche), anti-YAP rabbit polyclonal antibody, anti–phospho-YAP(Ser127) rabbit polyclonal antibody, anti-PUMA rabbit polyclonal antibody, anti-p21 mouse monoclonal antibody (Cell Signaling, Beverly, MA), anti-p73 mouse monoclonal antibody (Ab-4; Lab Vision, Fremont, CA), antiactin goat polyclonal antibody (Santa Cruz Biotechnology, Santa Cruz, CA), HRP conjugated anti–mouse IgG and anti–rabbit IgG (GE Healthcare, Uppsala, Sweden), and anti–goat IgG (Santa Cruz Biotechnology). Anti-Kpm rabbit polyclonal antibody was generated in our laboratory as described previously.[18] For immunoprecipitation assay, cells were lysed on ice for 30 minutes with Triton X–based lysis buffer (50 mM Tris-HCl at pH 8.0, 150 mM NaCl, 1% Triton X, 1 mM PMSF, 1 mM EDTA, and protease inhibitor cocktail; Nacalai Tesque), with the optional addition of phosphatase inhibitor cocktail 1 and 2 (Sigma-Aldrich) to detect phosphorylation status of YAP. The lysate, after centrifugation and precleaning, was incubated with 1 μg indicated antibodies overnight at 4°C and precipitated with protein G–sepharose beads (GE Healthcare) at 4°C for 3 hours. After washing 5 times with lysis buffer, the precipitate was boiled in 2 × sample buffer. Phosphatase treatment of the immunoprecipitates was done by incubating beads with 0.2 U/μL calf intestine phosphatase (CIP; Sigma-Aldrich) in 10 μL of 100 mM Tris-HCl (pH 8.0) at 37°C for 1 hour. Western blotting was performed according to the manufacturer's protocol for each antibody, and the protein bands were detected using the enhanced chemiluminescence (ECL) detection system (GE Healthcare).

Immunofluorescence microscopy

KG-1a cells were treated with 0.1 μg/mL ETP for 2.5 days. Then cells were cytospun on glass slides and fixed in ice-cold acetone for 3 minutes. After blocking, cells were incubated with 4 μg/mL anti-p73 mouse monoclonal antibody (Lab Vision) or mouse control IgG (Santa Cruz Biotechnology) in 1% bovine serum albumin containing PBS for 1 hour at room temperature. After extensive wash, cells were incubated with Alexa Fluor-488–conjugated anti–mouse IgG (Invitrogen), and 4′,6-diamino-2-phenylindole (DAPI; Sigma-Aldrich) staining was finally performed. Analysis was performed with fluorescence microscopy BIOZERO B8-8100 (Keyence, Osaka, Japan) that was equipped with a camera as an all-in-one type and with objective lenses (4×/0.2 NA and 20×/0.75 NA). B2-Viewer versus 1.0 (Keyence) and B2-Analyzer BZ-HIA versus 3.5 (Keyence) were used for image acquisition and image processing, respectively.

Chromatin immunoprecipitation assay

Chromatin immunoprecipitation (ChIP) assay of p73 binding to sites in the PUMA promoter region was done using ChIP-IT enzymatic kits (Active Motif, Carlsbad, CA) according to the manufacturer's instructions. Briefly, cells were fixed with 1% formaldehyde for 10 minutes, lysed at 4°C for 30 minutes, homogenized by passing through 27-gauge needles, and centrifuged. Pelleted nuclei were then subjected to enzymatic sharing for the optimized time. One-tenth volume was stored as the input and the remaining was diluted and incubated with 2 μg anti-p73 antibody (Ab-4; Lab Vision) or control IgG (Santa Cruz Biotechnology) at 4°C overnight. Immune complexes were precipitated with protein G–sepharose beads. After intensive washes, beads were treated with elution buffer. The supernatants and the stored input solutions were reverse cross-linked and treated with RNase and proteinase K, and chromatin DNA was purified using the kit-included DNA minicolumns. The following PCR primers were used to amplify the *PUMA* gene promoter: 5′-tgactgggacccacagatcca-3′ (forward) and 5′-tccaggggaccctgttagtgag-3′ (reverse).

Results

Kpm/Lats2 is down-regulated in various leukemias

The down-regulation of Kpm/Lats2 has been linked to poor prognosis of ALL. To evaluate the significance of Kpm/Lats2 expression in other types of leukemia, we measured the expression level of Kpm/Lats2 by real-time PCR in leukemic cells that were available in our laboratory. The expression of Kpm/Lats2 was markedly decreased in all adult T-cell leukemia (ATL)–derived cell lines and all clinical samples from ATL patients in comparison with the normal counterpart $CD4^+$ T cells (Figure 1A). Similarly, down-regulation of Kpm/Lats2 was observed in one NK cell line and most of the clinical samples from patients with NK cell leukemia/lymphoma, compared with the normal counterpart $CD3^-$ $CD56^+$ NK cells (Figure 1B). Both types of leukemias are known to be clinically aggressive and resistant to conventional chemotherapy. In other leukemic cell lines derived from acute myeloid leukemia (AML) except for KG-1a, B-ALL (Burkitt leukemia), T-ALL, and T-chronic lymphocytic leukemia (T-CLL), the expression level of Kpm/Lats2 was very low or hardly detectable, compared with normal peripheral blood mononuclear cells (PBMCs; Figure S1, available on the *Blood* website; see the Supplemental Materials link at the top of the online article). These results suggest that the down-regulation of Kpm/Lats2 is rather common in hematologic malignancies and the degree of decrease may be associated with poor prognosis.

Down-regulation of Kpm/Lats2 by shRNA does not affect the growth rate in 2 different leukemic cell lines

To delineate the cellular changes caused by Kpm/Lats2 down-regulation in leukemic cells, we made pools of Kpm/Lats2-knockdown KG-1a cells, a myeloid cell line, and ED-40515$^+$ cells, an ATL-derived cell line, using Kpm/Lats2-specific shRNA expression retrovirus vector. The reason why we chose these cell lines was because KG-1a and ED-40515$^+$ expressed relatively high levels of Kpm/Lats2 among myeloid and lymphoid cell lines, respectively (Figure 1A; Figure S1). Real-time PCR analyses of Kpm/Lats2 mRNA revealed that the expression levels of Kpm/Lats2 in Kpm/Lats2-knockdown KG-1a cells and ED-40515$^+$ cells was approximately 20% and approximately 30% of basal levels,

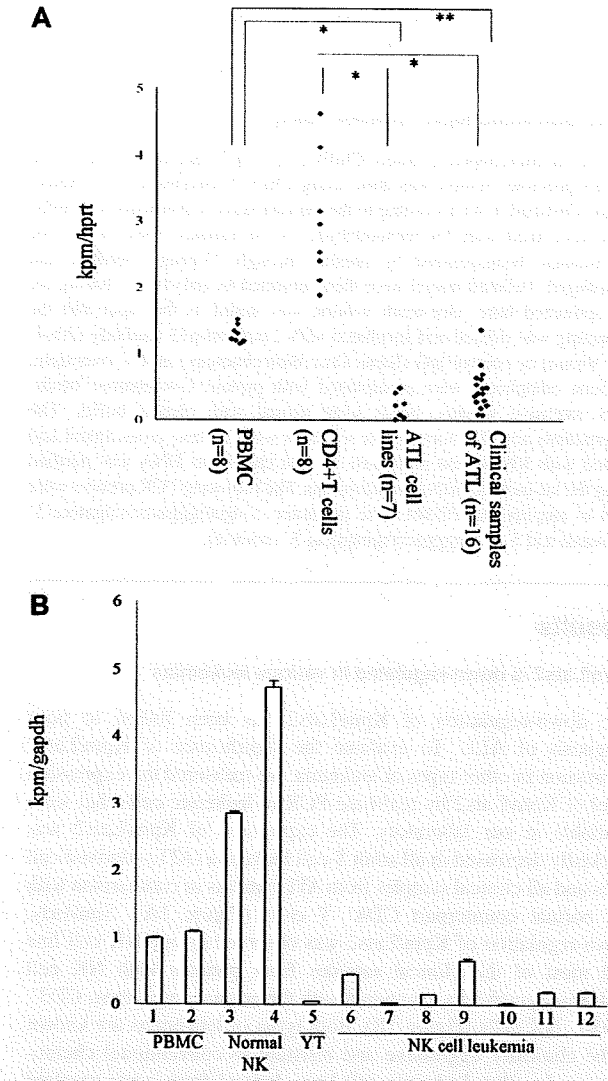

Figure 1. Quantitative analysis of Kpm/Lats2 mRNA in clinical samples and cell lines. (A) The amount of Kpm/Lats2 mRNA was measured in ATL cell lines, ATL clinical samples, normal PBMCs, and normal CD4+ T cells. Data normalized to hprt are shown representatively in scale that the value for normal PBMC is 1. Normalization to gapdh gave similar results. The highest one among the ATL cell lines represents ED-40515+. Analyses were performed in duplicate independently 3 times and representative data are shown (Welch *t* test: $*P < .001$; $**P < .005$). (B) The amount of Kpm/Lats2 mRNA was measured in NK cell line (YT), NK cell leukemia clinical samples, normal PBMCs (lanes 1-2), and normal $CD3^-56^+$ NK cells (lanes 3-4), NK cell line (YT; lane 5), and NK cell leukemia clinical samples (lane 6-12). Data normalized to gapdh are shown as mean plus or minus SD in scale that the value for normal PBMCs (lane1) is 1. Normalization to hprt gave similar results. Analyses were performed in triplicate independently twice, and representative data are shown.

respectively. There was no difference in the expression level of Lats1, the other human homologue of *Drosophila* Wts/Lats, between Kpm/Lats2-knockdown cells and wild-type or control cells (Figure 2A). We confirmed that Kpm/Lats2 expression was decreased also at the protein level in Kpm/Lats2-knockdown cells with Western blotting (Figure 2B).

Next we analyzed the growth rates of wild-type, Kpm/Lats2-knockdown, and control KG-1a cells as well as ED-40515+ cells to determine whether the expression level of Kpm/Lats2 affected the duration of cell cycle. It has recently been reported that cell number of mouse embryonic fibroblasts (MEFs) from Kpm/Lats2 knockout mouse (Kpm/$Lats2^{-/-}$) was approximately 1.25-fold more than those from wild-type mouse (Kpm/$Lats2^{+/+}$) at day 4.[27] Contrary to this, there was no difference between growth rate of Kpm/Lats2-knockdown cells and that of wild-type or control cells during 96 hours as measured by MTT assay (Figure 2C) and cell counting assay with trypan blue dye exclusion (data not shown).

Down-regulation of Kpm/Lats2 by shRNA in 2 different leukemic cell lines renders them resistant to DNA damage–inducing agents

To address whether down-regulation of Kpm/Lats2 renders leukemic cells resistant to DNA damage–inducing agents, we measured the cell viability of wild-type, Kpm/Lats2-knockdown, and control cells by MTT assay after the treatment with anticancer drugs, doxorubicin (DXR) or etoposide (ETP), which are used in standard chemotherapy for leukemia. The viability of these cells decreased after treatment of DXR or ETP in a dose-dependent and time-dependent manner but that of Kpm/Lats2-knockdown KG-1a cells was approximately 20% to 30% higher than that of wild-type or control KG-1a cells (Figure 2D). This tendency was also observed in ED-40515+ cells, although the proportion of dead cells increased faster and the difference in viability was slightly smaller than in KG-1a cells (Figure 2E). In addition, flow cytometric analysis with annexin V–PI dual staining revealed that treatment with ETP induced fewer apoptotic or dead cells in Kpm/Lats2-knockdown KG-1a cells than in control cells (Figure S2). Similar results were obtained with KG-1a cells transduced with microRNA-373,[52] which is known to down-regulate Kpm/Lats2 or those transfected with Kpm/Lats2-specific siRNA, although these reagents down-regulated Kpm/Lats expression less efficiently than the shRNA-expressing retrovirus vector (Figure S3A,B). These results clearly indicate that down-regulation of Kpm/Lats2 renders leukemic cells resistant to DNA damage.

Down-regulation of Kpm/Lats2 inhibits transcriptional induction of p21 and PUMA without affecting the IAP family members

We next examined the expression of several key molecules involved in cell survival. We searched for those genes whose expression level in Kpm/Lats2-knockdown KG-1a cells was significantly different from that in control cells after DNA damage stress. Two genes, p21 and PUMA, were identified by real-time PCR analysis–based screening. The expressions of p21 and PUMA were clearly induced by DNA damage–inducing agents in control KG-1a cells, although KG-1a line was p53 null,[53] whereas their inductions were strongly inhibited in Kpm/Lats2-knockdown KG-1a cells (Figure 3A). This finding was also confirmed at the protein level (Figure S4). Since p21 induces cell-cycle arrest[54] and PUMA can make Bax localize onto mitochondrial membrane to trigger apoptosis,[55,56] these results seemed to be in agreement with what we observed in cell viability assay. On the other hand, none of the members of the IAP family, the major inhibitors of apoptosis,[57] was up-regulated by silencing of Kpm/Lats2 despite treatment with ETP (Figure 3B). Of note is that in *Drosophila* the Hippo signals end up with the inhibition of Yki leading to apoptosis via down-regulation of Diap1.[7] In addition, although Bcl-2 was reportedly decreased by ectopic expression of Kpm/Lats2,[22] there was no significant difference in its expression level between Kpm/Lats2-knockdown and control cells (Figure 3B).

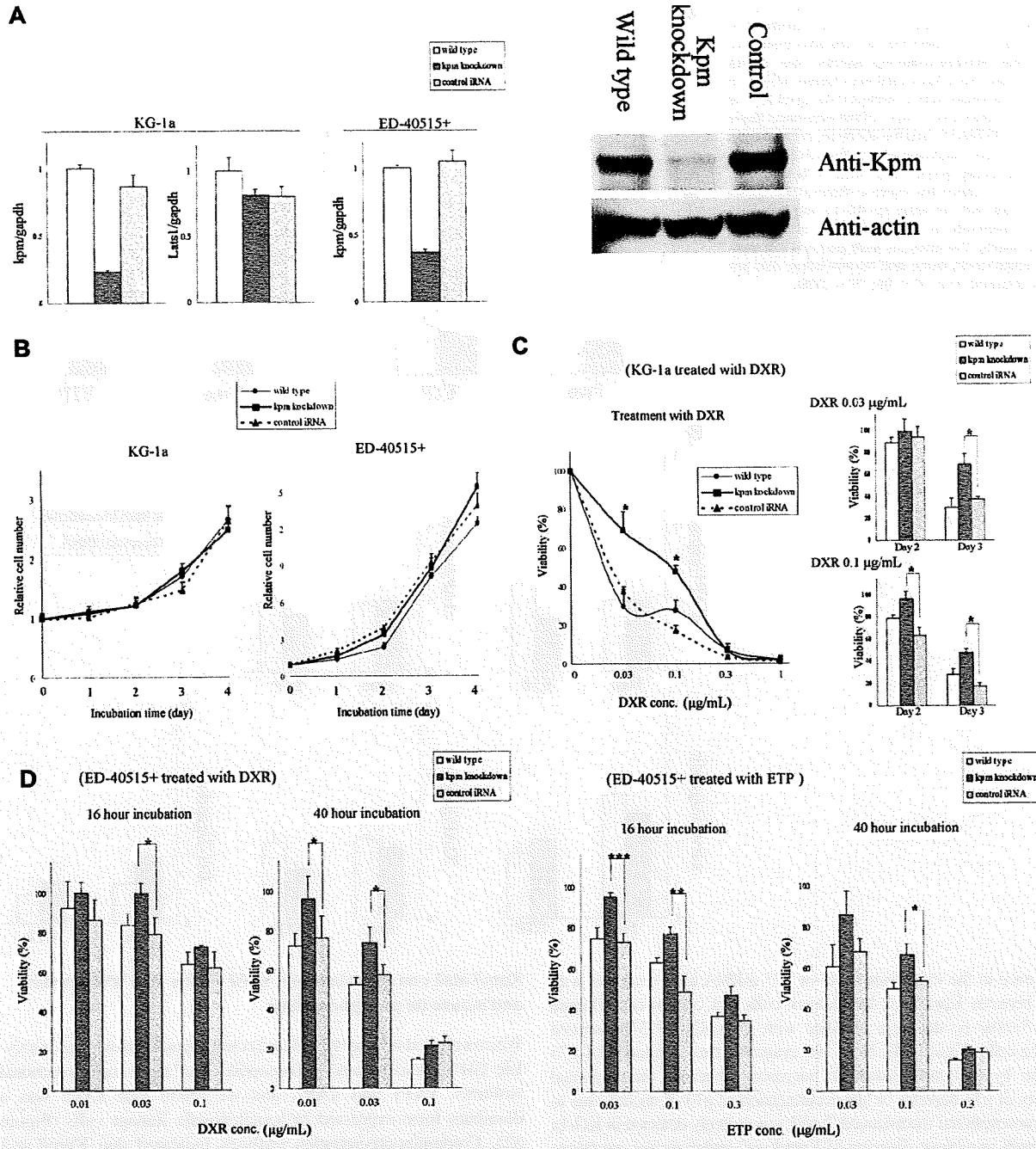

Figure 2. Down-regulation of Kpm/Lats2 renders cells resistant to DNA damage–inducing agents. (A) Kpm/Lats2-knockdown cells were established in KG-1a or ED-40515$^+$ cells using retrovirus (RV) vector containing Kpm/Lats2-specific shRNA. Wild type represents non–RV-transduced cells and control iRNA represents control shRNA-containing RV–transduced cells. Efficiency of Kpm/Lats2-specific shRNA was measured by real-time PCR analyses. Data normalized to gapdh are shown as mean plus or minus SD in scale that the value for wild type is 1. Analyses were performed in triplicate independently twice and representative data are shown. Western blot analysis of Kpm/Lats2 in wild-type, knockdown, or control cells in KG-1a. Analyses were performed independently twice and representative data are shown. (B) Simple growth curve without agents was measured by MTT assay. The assays were performed in quadruplicate independently 3 times and representative data are shown as mean plus or minus SD. (C) Cell viability after treatment with doxorubicin (DXR) or etoposide (ETP) in each KG-1a line was measured by MTT assay. The assays were performed in quadruplicate independently 3 times and representative data are shown as mean plus or minus SD (Welch *t* test: $^*P < .01$; $^{**}P < .05$). (D) Cell viability after treatment with DXR or ETP in each ED-40515$^+$ line was measured by MTT assay (Welch *t* test: $^*P < .05$; $^{**}P < .01$; $^{***}P < .005$). The assays were performed independently in quadruplicate 3 times, and representative data are shown as mean plus or minus SD.

Nuclear accumulation of p73 was suppressed in Kpm/Lats2-knockdown cells

We considered p73 as a molecule that replaced p53 in p53-null cells such as KG-1a and ED-40515$^+$ because p73 is a homologue of p53 and a transcriptional factor for p21 and PUMA expression. Therefore, we measured the amount of p73 at the protein level by Western blot analysis of whole-cell lysates. p73 was hardly detectable under normal conditions but became visible in control cells after treatment with ETP. In contrast, such increase in p73 protein was not observed in Kpm/Lats2-knockdown cells after the same treatment (Figure 4A). There was little